



ESA Climate Change Initiative Plus - Soil Moisture

Product Validation and Intercomparison Report (PVIR)

Supporting Product version v04.7

Deliverable ID: D4.1 Version 1

29 May 2020

Submitted by

EODC Earth Observation Data Centre for Water Resources Monitoring GmbH

The logo for EODC, with 'eodc' in a lowercase, sans-serif font. The 'e' is blue, 'o' is brown, and 'dc' is a lighter brown.

in cooperation with

TU Wien, VanderSat, ETH Zürich, and CESBIO



The logo for ETH zürich, with 'ETH' in a bold, italicized, black, sans-serif font and 'zürich' in a black, sans-serif font.



This document was compiled for the European Space Agency (ESA) CCI+ PHASE 1 - NEW R&D ON CCI ECVS Soil Moisture Project (ESRIN Contract No. 4000126684/19/I-NB).

For more information on the CCI programme of the ESA see <http://www.esa-cci.org/>.

Number of pages: 41 (including cover and preface)

| Authors: | M. Hirschi, N. Nicolai-Shaw*, W. Preimesberger, T. Scanlon, W. Dorigo, N. Rodriguez Fernandez, H. Thevenon, R. Kidd *as contributor of ESA CCI Phase 2 PVIR | | |
|-------------------------|--|---|--|
| Circulation (internal): | Project consortium and science partners | | |
| External: | ESA | | |
| Issue | Date | Details | Editor |
| 0.1 | 05.03.2020 | Document created based on the ESA CCI Phase 2 PVIR (Revision 3, version 2.6 from 29 Nov. 2018) Inclusion of validation results for ESA CCI SM v4.7 | M. Hirschi |
| 0.2 | 09.04.2020 | Inclusion of TUW and CESBIO input | M. Hirschi |
| 0.3 | 09.04.2020 | Minor corrections | M. Hirschi |
| 0.4 | 27.04.2020 | Format cover page, document information, update headers (all sections) format paging. Revision of Acronym table. Document Review. Release to ESA for review | R. Kidd |
| 0.5 | 04.05.2020 | Responding to RID's – provided in ESA_CCI_SM_D4.1_v1_PVIR_v4.7_issue_0.4_RID.docx, Revised Document Name, (RID, 001) Re-sized figure 3 (RID 007). To ETH for completion | R. Kidd |
| 0.6 | 14.05.2020 | Responding to RID's and implementation of changes as specified in the responses | M. Hirschi, W. Preimesberger, N. Rodriguez Fernandez |
| 1.0 | 29.05.2020 | Accepted all reviewers comments. Closed document. Prepared to pdf for delivery | R. Kidd |

For any clarifications please contact Martin Hirschi (martin.hirschi@env.ethz.ch).



Project Partners

Prime Contractor, Project Management **EODC**, Earth Observation Data Centre for Water Resources Monitoring (Austria)

Earth Observation Partners **TU Wien**, Vienna University of Technology (Austria)
VDS, Vandersat The Netherlands)
CESBIO, CESBIO (France)

Climate Research Partner **ETH Zürich**, Institute for Atmospheric and Climate Science, (Switzerland)

Table of Contents

| | | |
|----------|--|-----------|
| 1 | EXECUTIVE SUMMARY | 1 |
| 2 | DOCUMENTS..... | 2 |
| 2.1 | APPLICABLE DOCUMENTS | 2 |
| 2.2 | REFERENCE DOCUMENTS..... | 3 |
| 2.3 | BIBLIOGRAPHY | 3 |
| 3 | INTRODUCTION..... | 4 |
| 3.1 | PURPOSE OF THE DOCUMENT | 4 |
| 3.2 | TARGET AUDIENCE | 4 |
| 3.3 | IMPORTANT DOCUMENTS | 4 |
| 4 | DATASETS OVERVIEW | 5 |
| 5 | VERIFICATION AND VALIDATION RESULTS | 5 |
| 5.1 | VERIFICATION AND BASIC VALIDATION OF THE PRODUCT (TU WIEN) | 5 |
| 5.1.1 | <i>Datasets</i> | 5 |
| 5.1.2 | <i>Dataset completeness</i> | 7 |
| 5.1.3 | <i>Validation with in-situ reference data.....</i> | 9 |
| 5.1.4 | <i>Validation with model reference data.....</i> | 11 |
| 5.1.5 | <i>Summary</i> | 12 |
| 5.2 | COMPARISON TO IN-SITU OBSERVATIONS FROM ISMN AND GLOBAL LAND REANALYSIS PRODUCTS (ETH ZÜRICH) 13 | |
| 5.2.1 | <i>Datasets and data processing</i> | 13 |
| 5.2.2 | <i>General findings</i> | 15 |
| 5.2.3 | <i>The influence of measuring depth</i> | 18 |
| 5.2.4 | <i>The influence of land cover.....</i> | 19 |
| 5.2.5 | <i>Temporal subsets and product evolution</i> | 20 |
| 5.2.6 | <i>Summary</i> | 21 |
| 6 | VALIDATION ACTIVITIES TOWARDS FUTURE ALGORITHM DEVELOPMENT | 22 |
| 6.1 | EVALUATION OF DIFFERENT SMOS AND SMAP ALGORITHMS WITH RESPECT TO GLDAS (CESBIO).. | 22 |
| 6.1.1 | <i>Datasets and data processing</i> | 22 |
| 6.1.2 | <i>Evaluation with respect to in-situ measurements.....</i> | 22 |
| 6.1.3 | <i>Comparison of the temporal dynamics with respect to GLDAS.....</i> | 23 |
| 6.1.4 | <i>Comparison of the Cumulative Distribution Functions.....</i> | 24 |
| 6.1.5 | <i>Summary</i> | 28 |
| 7 | CONCLUSIONS..... | 29 |



8 **BIBLIOGRAPHY** **30**



List of Figures

Figure 1 : 571 ISMN stations used for the internal validation of ESA CCI SM v04.7, only sensors between 0 and 5 cm depth are considered 6

Figure 2 : Hovmoeller diagram of fractional number of valid observations per month in the Soil Moisture variable of ESA CCI SM v04.5 COMBINED (top) and ESA CCI SM v04.7 COMBINED (bottom). 7

Figure 3: Monthly soil moisture Uncertainty in ESA CCI SM v04.7 (COMBINED) 8

Figure 4: Change in number of (daily) observations in ESA CCI SM between v04.5 and v04.7 for the ACTIVE (top), COMBINED (middle) and PASSIVE (bottom) product..... 9

Figure 5: Intercomparison of Pearson's R between ESA CCI SM v04.5 and v04.7 (ACTIVE, COMBINED, PASSIVE) with ISMN SM observations as the reference 10

Figure 6: Intercomparison of Pearson's ubRMSD between ESA CCI SM v04.5 and v04.7 (ACTIVE, COMBINED, PASSIVE) with ISMN SM observations as the reference 10

Figure 7 : Intercomparison of Pearson's R (left) and ubRMSD (right) for the ACTIVE, COMBINED and PASSIVE product in ESA CCI SM v04.7 with respect to ISMN reference data..... 11

Figure 8 : Intercomparison of Pearson's R between ESA CCI SM v04.5 and v04.7 (ACTIVE, COMBINED, PASSIVE) with GLDAS Noah SM simulations as the reference..... 12

Figure 9 : Intercomparison of ubRMSD between ESA CCI SM v04.5 and v04.7 (ACTIVE, COMBINED, PASSIVE) with GLDAS Noah SM simulations as the reference..... 12

Figure 10: Overview of the spatial coverage of the stations considered in this study, rectangles indicate the four focus areas of the comparison, i.e., the United States (US, red), Europe (EU, blue), Africa (AF, green), and Australia (AUS, purple). Stations are color coded by network, see Figure 11 for the legend..... 14

Figure 11: Overview of the temporal coverage of the stations considered in this study, after masking for common data availability, split per region. The number of stations per region is indicated in brackets. 15

Figure 12: Correlation between in-situ soil moisture and ESA CCI SM for versions v0.1, v02.2, v03.3, and v04.7, as well as ERA5-Land soil moisture layer 1 (ERA5-Land l1, 0-7 cm), for absolute soil moisture (left) and the anomalies (right). 16

Figure 13: Correlation of the gridded soil moisture products as compared to in-situ station observations (5 cm depth) for three combinations of Köppen-Geiger classes (BSx - arid, Csx/Dsx - temperate/continental summer dry, Cfx/Dfx - temperate/continental without dry season). (Top row) Absolute values of soil moisture (ABS); (bottom row) inter-annual anomalies (IAA). Shown is the median and IQR of the correlations, n denotes the number of stations underlying the distributions. 17

Figure 14: As Figure 13, but showing ubRMSD. 18

Figure 15: Correlation between in-situ measurements for ESA CCI SM v0.1, v02.2, v03.3, v04.2, and v04.7, as well as ERA5-Land soil moisture layer 1 and 2 for the absolute soil moisture



values (top) and the anomalies (bottom). For each product, we distinguish between 3 regions US, EU, and AUS (red, blue and purple, AF has insufficient data coverage), and the correlation at 5 cm depth (circles) and 10 cm depth (triangles). The same number of stations is taken into account for the individual distributions of the top and bottom panels. The black circles/triangles represent the respective median values. 19

Figure 16: Correlation between in-situ measurements at 5 cm depth and ESA CCI SM v0.1, v02.2, v03.3, and v04.7, as well as ERA5-Land soil moisture layer 1, differentiating between grassland (orange) and forest (green) sites for absolute soil moisture values and anomalies. Black dot denotes the median value..... 20

Figure 17: Correlation of the gridded soil moisture products as compared to in-situ station observations in 5 and 10 cm depth for the full year for the US. Subdivided in consecutive 4-year periods (1997-2000, 2001-2004, 2005-2008, 2009-2012, and 2013-2016) as well as for the longest period data is available (1997-20.., end date would e.g. be 2010 for CCI v0.1, but is 2016 for e.g. CCI v4.1). Note that in this case, data is not masked for common data availability. Whiskers show the median and the IQR. Above indicated the number of stations correlations were calculated for that comply to the following criteria: at least 10% of the timeseries is not NA, p-value < 0.05, and the calculated correlation is positive. And below indicated the number of years considered. 21

Figure 18: Box plots for the standard deviation of the difference (STDD, left), the Pearson correlation (R, center) and the bias (remote sensing or model minus in-situ, right) with respect to in-situ measurements from the SCAN (upper panels) and USCRN (lower panels) networks. The red line is the median of the distribution and the blue box represent the data within the 25th and the 75th percentile of the sample data (q1 and q3, respectively). The whiskers extend from $q3 + 1.5 \times (q3 - q1)$ to $q1 - 1.5 \times (q3 - q1)$. Samples outside this range are considered as outliers (red crosses). The datasets that are evaluated are GLDAS, SMOS L3 for ascending and descending orbits (SMOSL3 A and D), SMOS LPRM for ascending and descending orbits (SMOSLP A and D), SMOS Near-Real-Time (SMOSNRT), SMOS IC (SMOSIC A and D), SMAP Level 2 (SMAPL2) and SMAP LPRM for ascending and descending orbits (SMAPLP A and D)..... 23

Figure 19: Maps of the Pearson correlation with respect to GLDAS of the SMAP LPRM and SMOS CATDS L3, LPRM and IC for ascending orbits, the SMOS NRT and the SMAP Level 2 products. 24

Figure 20: Maps of the sum of absolute differences of the CDFs of SMOS and SMAP products with respect to the GLDAS CDF computed in 30 bins. 25

Figure 21: Blue circles and lines show the CDF for different SMOS and SMAP products while red circles and line shows the CDF for the GLDAS time series temporally interpolated at the acquisition times of each SMAP and SMOS products (for the closest grid point to longitude - 100° and latitude 40°)..... 26

Figure 22: Blue circles and lines show the CDF for different SMOS and SMAP products while red circles and line shows the CDF for the GLDAS time series temporally interpolated at the



acquisition times of each SMAP and SMOS products (for the closest grid point to longitude - 100° and latitude 65°)..... 27

Figure 23: Left: map of the CDF differences from SMOS IC ASC and GLDAS computed SMOS data only with dates after the launch of SMAP. Right: Blue circles and lines show the CDF for the SMOS IC ASC product computed from the launch date of SMAP while red circles and line shows the CDF for the GLDAS time series temporally interpolated at the acquisition times of SMOS (for the closest grid point to longitude -100° and latitude 40°). 28



List of Tables

| | |
|--|----|
| Table 1: Overview of the products used for the ESA CCI SM validation..... | 5 |
| Table 2: Median of all validation metrics derived from comparison to ISMN SM for ESA CCI SM v04.7 and v04.5 (ACTIVE, COMBINED and PASSIVE product)..... | 10 |
| Table 3 : Median of all validation metrics derived from comparison to GLDAS Noah SM for ESA CCI SM v04.7 and v04.5 (ACTIVE, COMBINED and PASSIVE product)..... | 11 |



Acronyms

| | |
|---------|---|
| ABS | Absolute soil moisture |
| AMSR-E | Advanced Microwave Scanning Radiometer - Earth Observing System |
| ASAR | Advanced Synthetic Aperture Radar |
| ASCAT | Advanced SCATterometer |
| ATBD | Algorithm Development Document |
| CAL-VAL | Calibration and validation |
| CDF | Cumulative Distribution Function |
| CCI | Climate Change Initiative |
| DA | Data Assimilation |
| ECMWF | European Centre for Medium Range Weather Forecasts |
| ENVISAT | Environmental Satellite |
| ECV | Essential Climate Variable |
| CCI SM | Soil moisture time series developed in framework of ESA CCI |
| EO | Earth Observation |
| ERA | ECMWF Re-Analysis |
| ESA | European Space Agency |
| ISMN | International soil moisture network |
| LSM | Land surface model |
| LTA | Long-term anomaly of soil moisture |
| NASA | National Aeronautics and Space Administration |
| NCAR | National Center for Atmospheric Research |
| NH | Northern Hemisphere |
| PSD | Product Specification Document |
| PVIR | Product Validation and Intercomparison Report |
| PVP | Product Validation Plan |
| RMSD | Root mean square difference |
| RMSE | Root mean square error |
| SAC-SMA | Sacramento Soil Moisture Accounting model |
| SM | Soil moisture |
| SMAP | Soil Moisture Active Passive mission |
| SMOS | Soil Moisture and Ocean Salinity mission |
| SSM | Surface soil moisture |
| STA | Short-term anomaly of soil moisture |
| TUW | Vienna University of Technology |
| ubRMSD | Unbiased root mean square difference |
| VWC | Volumetric water content |
| WMO | World Meteorological Office |

1 Executive Summary

Within the framework of the European Space Agency (ESA) Climate Change Initiative (CCI) soil moisture project, a 40-year (1978-2019) soil moisture time series (ESA CCI SM v04.7) is developed, which consists of three products: an active data set, a passive data set and a combined data set. It provides daily surface soil moisture with a spatial resolution of 0.25° . The merged product as well as its active and passive sources are publicly available to the user on the project webpage (<http://www.esa-soilmoisture-cci.org>). Furthermore, the detailed description of its development (ATBD, RD-02), the product specification (PSD, RD-03), and a product user guide (PUG, RD-04) are publicly available on the project webpage (<http://www.esa-soilmoisture-cci.org>).

The validation of the final merged data set ESA CCI SM v04.7 is an important mechanism within the production process and is documented in this Product Validation and Intercomparison Report (PVIR). The guideline of the ESA CCI SM product validation is described in the Product Validation Plan (PVP, RD-06) and ensures that the validation meets the overall user requirements and that it is carried out in a transparent way. The established validation protocol is broadly accepted by the international soil moisture community. The validation is performed with in-situ or other appropriate global datasets (e.g., land surface models, land data assimilation systems, land reanalyses) that were not used for the production of the ESA CCI SM product. Additionally, the ESA CCI SM product releases undergo a basic “verification” as part of the production process, which is also documented in this PVIR.

The PVIR encompasses the following analyses (carried out independently by the indicated partners).

TU Wien: The product is verified for completeness, i.e. spatial and temporal coverage, and also with respect to the previous, approved (public), version. Basic validation with respect to a preselection of ISMN networks (0-5 cm depth) as well as comparison to GLDAS Noah v2.1 soil moisture is performed in terms of multiple validation metrics: MSE (mean-square error), R (Pearson’s correlation coefficient), Rho (Spearman’s correlation coefficient), Tau (Kendall rank correlation coefficient), and ubRMSD (unbiased root-mean-square-difference). Validations are performed globally and after bias correction by matching the mean and standard deviation of each ESA CCI SM time series to that of the reference series. In case of intercomparison between versions, only the common observations are used.

The evaluation shows only minimal differences compared to the last public version. Differences are found in terms of temporal coverage (due to the dataset extension) but also in terms of flagging of input datasets.

ETH Zürich: After Verification, the ESA CCI SM products (from v0.1 up to the latest ESA CCI SM product release, v04.7) are validated over four regions (North America, Europe, Sub-Saharan Africa, and Australia) and globally using in-situ observations from the ISMN and using the ERA5-Land and ERA-Interim/Land soil moisture reanalyses at 0.25° resolution. This evaluation uses the two top layers of the ERA soil moisture reanalyses (i.e., 0-7 cm and 7-28 cm depths) to compare the ESA CCI SM products, and the in-situ observations in 5 and 10 cm depth.

The evaluation shows no clear regions where the ESA CCI SM products agree very well or very poorly with in-situ observations. However, the highest and most consistent correlations were found over Australia where the in-situ observations were located in the same climatic region. The ESA CCI SM products correlate higher with the observed in-situ soil moisture at 5 cm than at 10 cm depth. This distinction in moisture at different depths was less clear for the comparison with ERA5-Land. Over the US, the ESA CCI SM products show consistently higher correlation with the in-situ observations in areas of grassland than compared to areas of forest vegetation cover. This distinction for different vegetation types is less clear for the comparison with the ERA5-Land reanalysis.

CESBIO: For support of future algorithm development, the possible impacts of replacing the GLDAS Noah v2.1 model as reference for the rescaling of other time series by matching their Cumulative Distribution Functions (CDFs) is investigated. For this, four SMOS and two SMAP datasets computed using different algorithms were compared to GLDAS. Evaluations of SMOS, SMAP and GLDAS soil moisture was performed with respect to in-situ measurements from the SCAN and USCRN networks over the Continental United states of America (CONUS). In addition, the temporal dynamics of the remote sensing datasets were compared to that of the GLDAS model by computing Pearson correlation maps. Finally, the CDFs of the different time series were computed and two metrics were studied to visualize the CDF differences in a map and to study the spatial distribution of the CDF differences in order to understand where the impacts of replacing GLDAS by an L-band dataset would be the most significant. The regions where both the temporal dynamics and the CDFs differ the most with respect to GLDAS are the Equatorial forest and the high northern latitudes. These are the regions where changing the reference dataset for the rescaling will have a higher impact. The impact of the length of the time series used to compute the CDF was evaluated and it was shown that using only the shorter time period for which SMAP is available does not affect significantly the CDF computation. The SMOS CATDS Level 3 product shows lower performance with respect to in-situ measurements and higher differences to GLDAS than the other three SMOS datasets. SMAP data are available in some regions where SMOS data are more affected by radio frequency interferences. Otherwise, it is not obvious to choose one or the other L-band datasets only with the results of this study.

2 Documents

2.1 Applicable documents

The documents outlined below detail the scope and focus for the work reported in this document.

[AD-1] ESA CCI+ PHASE 1 - NEW R&D ON CCI ECVS Soil Moisture Project Contract No: 4000126684/19/I-NB.

[AD-2] Climate Change Initiative Extension (CCI+) Phase 1 New R&D on CCI ECVs, Statement of Work, ESA Earth Observation Directorate, ESA-CCI-EOPS-PRGM-SOW-18-0118.



2.2 Reference documents

This section provides a list of reference documents either on which we base this document, or to which this document refers.

[RD-01] Product Validation and Intercomparison Report (PVIR), revision 3, version 2.6, 29 Nov. 2018

[RD-02] Algorithm Theoretical Basis Document (ATBD), v4.7, Mar. 2020

[RD-03] Product Specification Document (PSD), v4.7, Mar. 2020

[RD-04] Soil Moisture CCI Product User Guide (PUG), v4.7, Mar. 2020

[RD-05] Climate Research Data Package (CRDP), v4.7, Mar. 2020

[RD-06] Product Validation Plan (PVP), version 1.2, 14 Aug. 2019

2.3 Bibliography

A complete bibliographic list, detailing scientific texts or publications that support arguments or statements made in this document is provided in Section 8.



3 Introduction

3.1 Purpose of the document

The purpose of the PVIR is the final validation of the soil moisture time series, which is developed in the framework of the ESA CCI soil moisture project. It includes the verification and the validation of the product as outlined in the PVP.

3.2 Target audience

This document targets users of the soil moisture time series produced, as well as the scientific community. It demonstrates the value of an intercomparison between the ESA CCI SM product and other available soil moisture products.

3.3 Important documents

Detailed information on the ESA CCI SM v04.7 time series is provided in the Algorithm Development Document (ATBDv4.7), the Product Specification Document (PSDv4.7), as well as the Product User Guide (PUGv4.7), produced in the framework of the ESA CCI soil moisture project. These documents are listed in Section 2 and are publicly available on the project webpage (<http://www.esa-soilmoisture-cci.org>).

4 Datasets overview

The following table shows an overview of the datasets used for the validation of the ESA CCI SM product. For details on the single ESA CCI SM product versions, please refer to the CDRP [RD-05].

Table 1: Overview of the products used for the ESA CCI SM validation.

| Product | Producer | Data class | Description | Period | Coverage |
|------------------|--|--------------------------------|---|-------------------------------------|---|
| ISMN | Individual soil moisture networks, hosted at TU Wien | In-situ | In-situ soil moisture measurements | January 1950-present and continuing | Global (but only few data in South America, Africa, and Asia) |
| ERA5-Land | ECMWF | Land surface model reanalysis | Reanalysis data for volumetric soil water at different levels of the soil profile | 1981-2019 (current availability) | Global |
| ERA-Interim/Land | ECMWF | Land surface model reanalysis | Reanalysis data for volumetric soil water at different levels of the soil profile | 1979-2010 | Global |
| GLDAS Noah v2.1 | NASA | Land surface model simulations | Model simulations for volumetric soil water at different levels of the soil profile | 2000-2019 | Global |

5 Verification and validation results

The following sections present the verification and validation results of the ESA CCI SM v4.7 product.

5.1 Verification and basic validation of the product (TU Wien)

As part of the product generation, verification and basic validation activities are carried out. The generated dataset was evaluated for completeness and compared to various reference datasets to ensure the physical plausibility of the SM products generated.

5.1.1 Datasets

In addition to the newly generated v04.7 datasets of ESA CCI SM, the previous public release (v04.5) was used. All three respective products of ESA CCI SM (ACTIVE, PASSIVE, COMBINED) were inter-compared to in-situ and model reference data.

ISMN station measurements

Ground based measurements of the International Soil Moisture Network (ISMN) available in depths between 0 and 5 centimetres of networks shown in Figure 1 were used (full download from 11 December 2019). Most stations that were considered are found within the United

States. In total 571 ISMN time series are considered, depending on the spatial and temporal overlap with ESA CCI SM, less time series might be used in the actual validation process. ISMN observations are filtered based on the provided quality flags. Only values flagged as “good” are used to exclude e.g. measurements when soil temperature is $<0^{\circ}\text{C}$. ESA CCI SM and ISMN SM observations are temporally matched during validation (the temporally closest observations are compared) using a window of 1 hour before/after the reference measurement time stamp. For each ISMN station the spatially closest ESA CCI SM pixel is used (which leads to over-representation of some pixels in the validation results) with a maximum lookup distance of 30 km. Biases between in-situ and satellite SM are corrected by matching the mean and standard deviation of each time series. The time period for validation depends on the time period covered by an ISMN station.

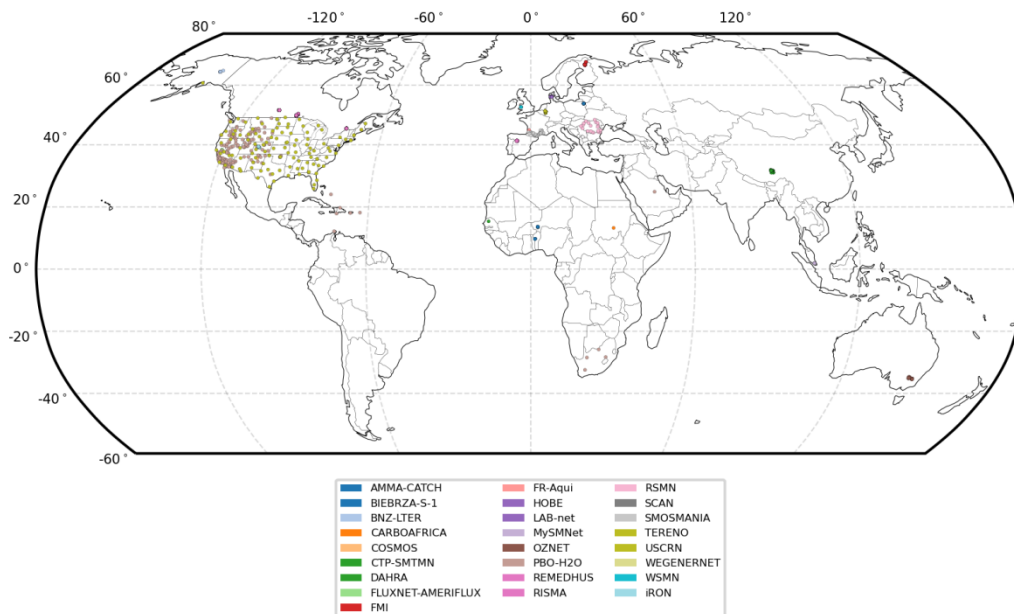


Figure 1 : 571 ISMN stations used for the internal validation of ESA CCI SM v04.7, only sensors between 0 and 5 cm depth are considered

GLDAS Noah

As the second reference data source, soil moisture simulations from version 2.1 of the GLDAS Noah model are used (Rodell et al. 2004). The “SoilMoi0_10cm_inst” variable is representative of water in the top soil layer (0-10cm). GLDAS Noah is also used in the production of ESA CCI SM as a scaling reference for the COMBINED product as well as for Triple Collocation (TC) analysis in the merging scheme. Validation results are therefore not completely independent. Issues in the product generation such as data loss would however still be noticeable. GLDAS Noah v2.1 is available in the period from 2000-01-01 until 2019-12-31. The original data is in units of $[\text{kg}/\text{m}^2]$ and values range from 0 and 100.

5.1.2 Dataset completeness

Figure 2 : Hovmoeller diagram of fractional number of valid observations per month in the Soil Moisture variable of ESA CCI SM v04.5 COMBINED (top) and ESA CCI SM v04.7 COMBINED (bottom). shows the fractional coverage of ESA CCI SM COMBINED observations over time and latitude. The increase in coverage due to more available sensors over time is clearly visible. The number of observations is comparable to the previous version (v04.5, Figure 2 : Hovmoeller diagram of fractional number of valid observations per month in the Soil Moisture variable of ESA CCI SM v04.5 COMBINED (top) and ESA CCI SM v04.7 COMBINED (bottom). top). Figure 2 : Hovmoeller diagram of fractional number of valid observations per month in the Soil Moisture variable of ESA CCI SM v04.5 COMBINED (top) and ESA CCI SM v04.7 COMBINED (bottom). (bottom) therefore indicates that no data was lost during the production of v04.7. The addition of data for the year 2019 is also obvious and in line with previous years in terms of fractional coverage.

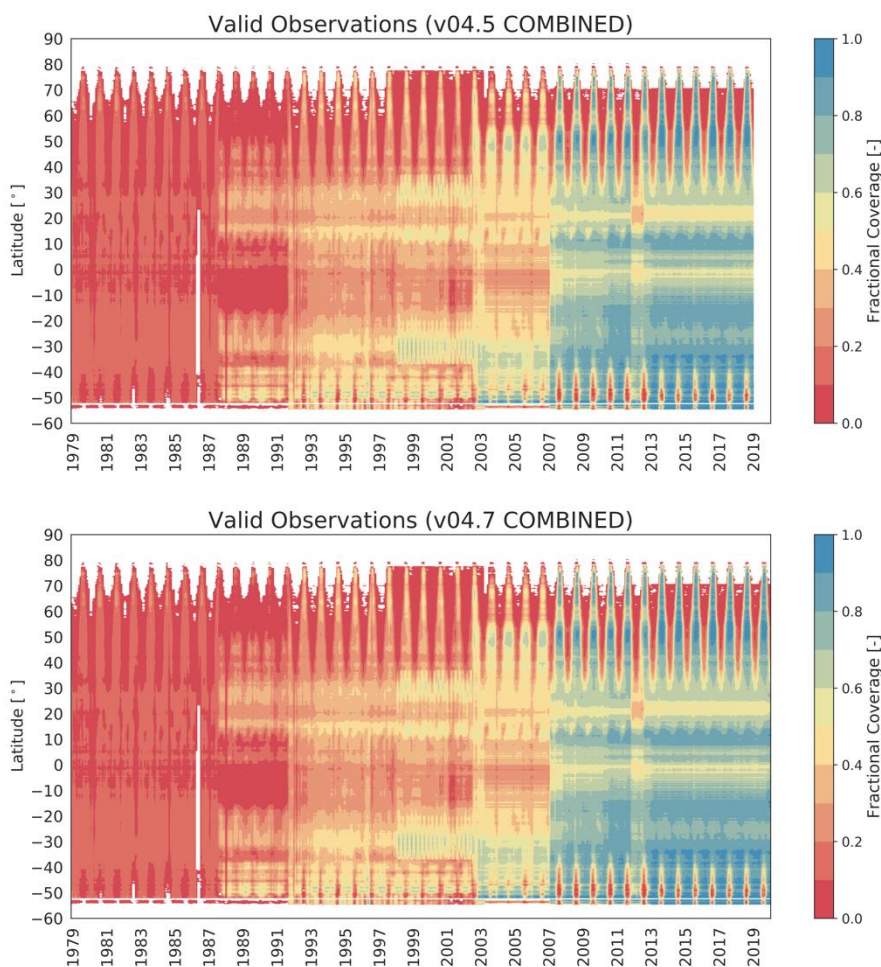


Figure 2 : Hovmoeller diagram of fractional number of valid observations per month in the Soil Moisture variable of ESA CCI SM v04.5 COMBINED (top) and ESA CCI SM v04.7 COMBINED (bottom).



Figure 3 shows changes in the uncertainty variable in ESA CCI SM v04.7 COMBINED over time/latitude. Uncertainty values are only provided after the year 1987.

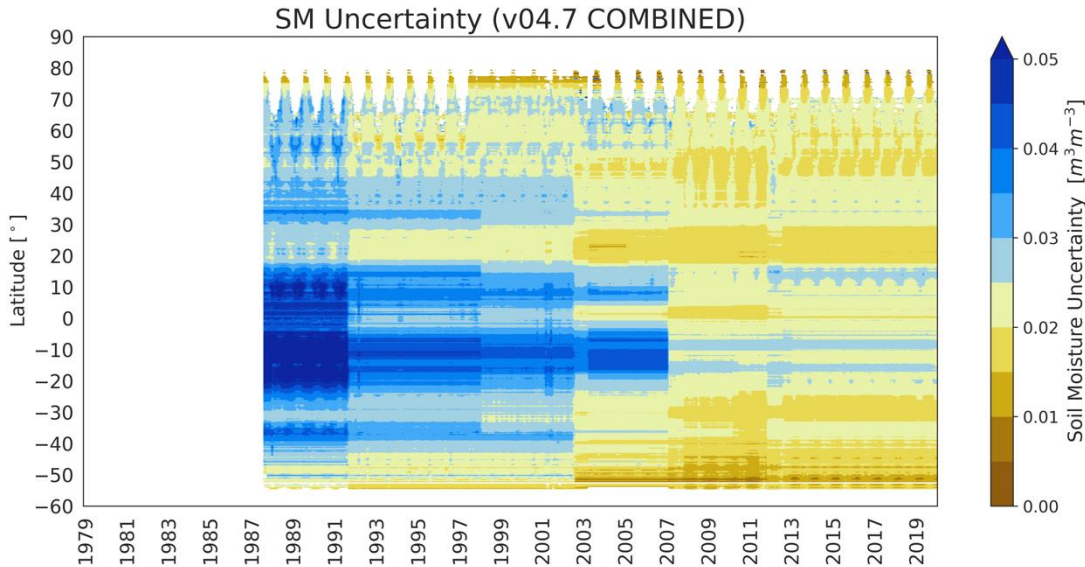


Figure 3: Monthly soil moisture Uncertainty in ESA CCI SM v04.7 (COMBINED)

Figure 4 contains maps to show the increase in number of observations in the ACTIVE, COMBINED and PASSIVE product of ESA CCI SM v04.7 compared to the previous public version (v04.5). As expected, for most areas between 0 and 365 observations were added due to the temporal extension of one year. Some areas in the ACTIVE product show an increase in data of more than that, which is due to changes in the flagging of H SAF ASCAT SSM. This also applies to other, currently operating sensors (SMOS, AMSR2), for which the most up-to-date dataset version is used when a new version of ESA CCI SM is generated. For the same reason also in the PASSIVE and COMBINED product, some pixels show an increase in data coverage of more than 365 values or even a decrease compared to last year's version.

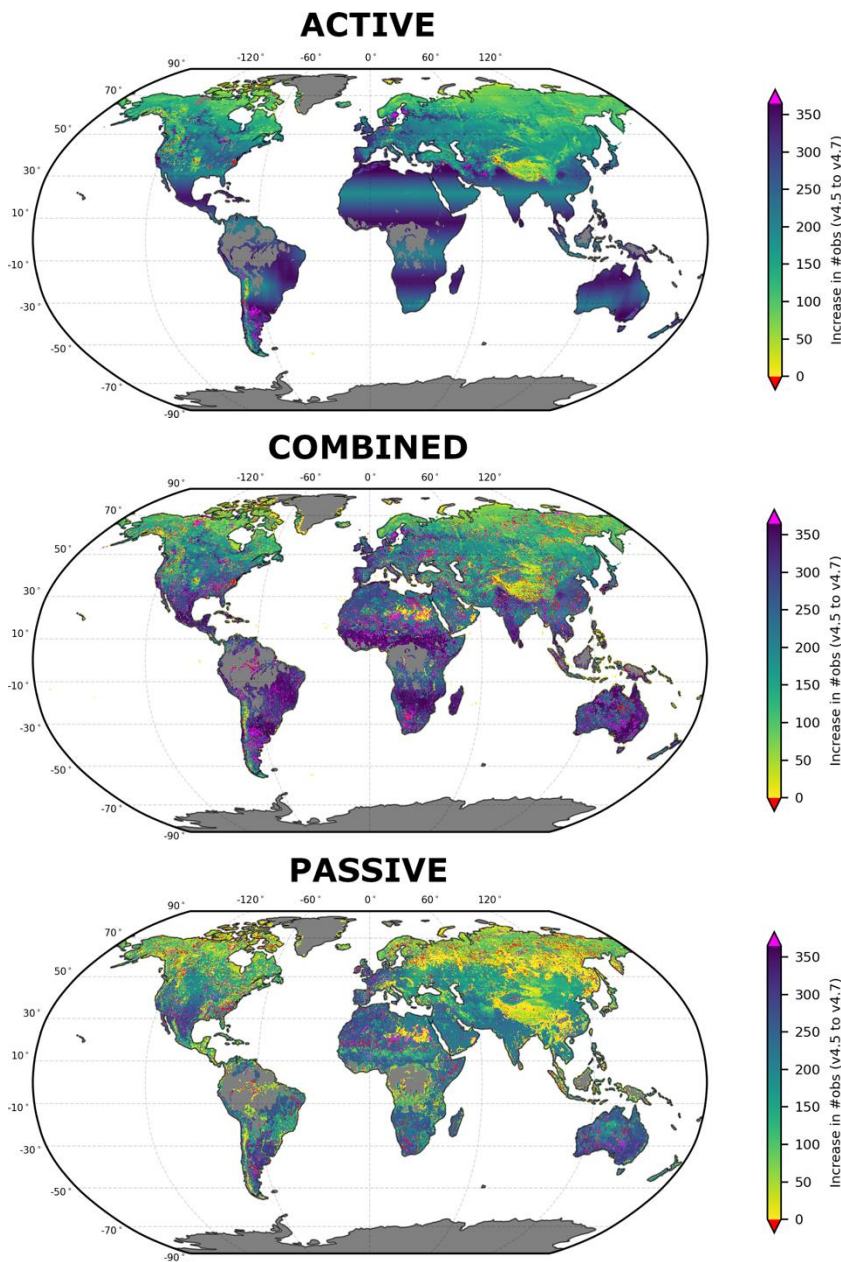


Figure 4: Change in number of (daily) observations in ESA CCI SM between v04.5 and v04.7 for the ACTIVE (top), COMBINED (middle) and PASSIVE (bottom) product.

5.1.3 Validation with in-situ reference data

Version intercomparison

Figure 5 shows the intercomparison of Pearson's R between ESA CCI SM v04.5 and v04.7 for the three products with respect to ISMN soil moisture. "N" describes the number of considered time series in the box plot. Figure 6 shows the same for ubRMSD.

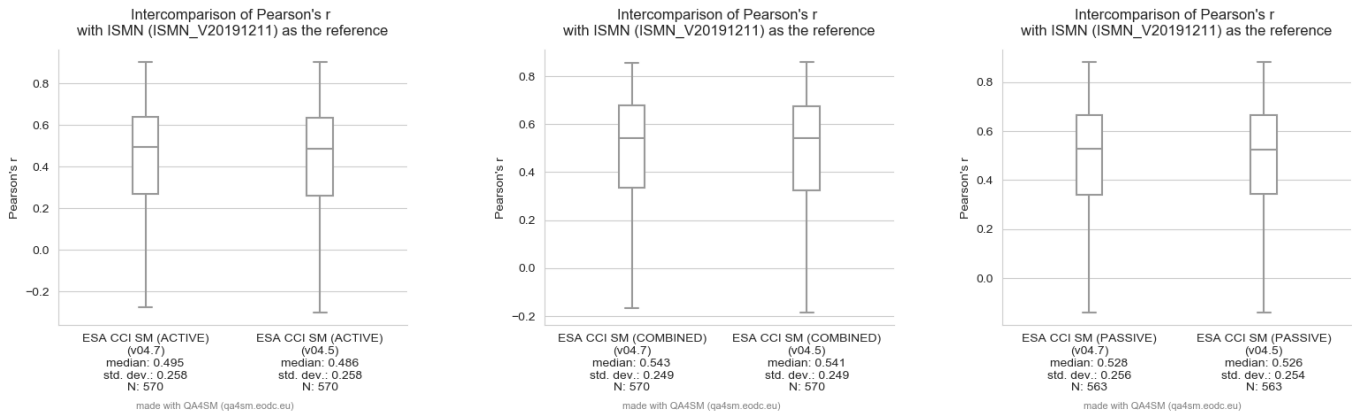


Figure 5: Intercomparison of Pearson's R between ESA CCI SM v04.5 and v04.7 (ACTIVE, COMBINED, PASSIVE) with ISMN SM observations as the reference

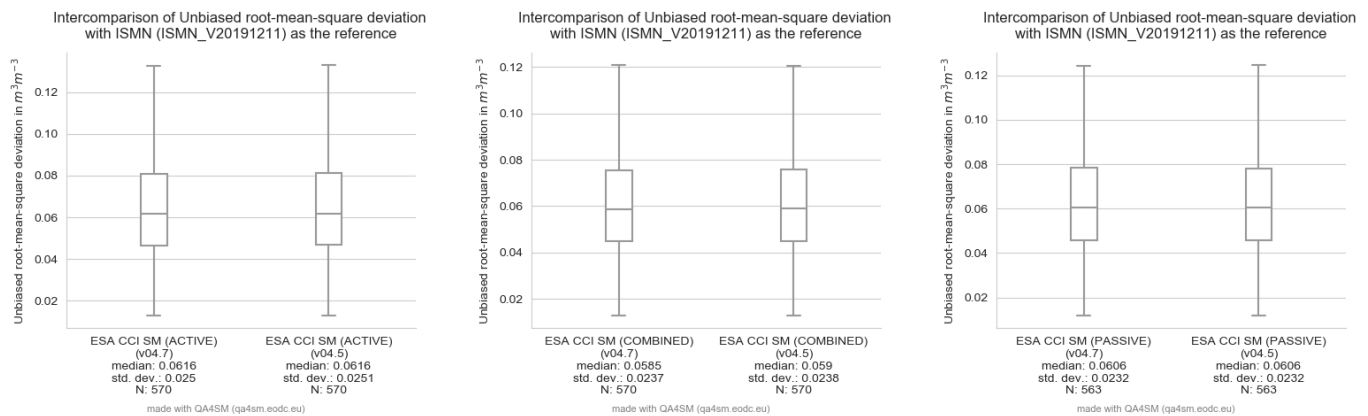


Figure 6: Intercomparison of Pearson's ubRMSD between ESA CCI SM v04.5 and v04.7 (ACTIVE, COMBINED, PASSIVE) with ISMN SM observations as the reference

Only minor changes between the versions are found, which is expected as no algorithmic changes were introduced between the two versions. Table 2 shows the difference in the median of all calculated metrics.

| Metric | ACTIVE | | COMBINED | | PASSIVE | |
|--|--------|--------|----------|--------|---------|--------|
| | v04.5 | v04.7 | v04.5 | v04.7 | v04.5 | v04.7 |
| MSE [m ³ /m ³] | 0.0004 | 0.0004 | 0.003 | 0.003 | 0.004 | 0.004 |
| Pearson's R [-] | 0.486 | 0.495 | 0.541 | 0.543 | 0.526 | 0.528 |
| Spearman's R [-] | 0.484 | 0.4890 | 0.557 | 0.556 | 0.546 | 0.546 |
| ubRMSD [m ³ /m ³] | 0.0616 | 0.0616 | 0.059 | 0.0585 | 0.0606 | 0.0606 |
| Kendall Tau [-] | 0.34 | 0.342 | 0.395 | 0.397 | 0.386 | 0.386 |

Table 2: Median of all validation metrics derived from comparison to ISMN SM for ESA CCI SM v04.7 and v04.5 (ACTIVE, COMBINED and PASSIVE product).

Product Intercomparison

To evaluate differences in the performance of the ACTIVE, COMBINED and PASSIVE product, an intercomparison with the same reference data was performed. As expected the COMBINED product performs best in terms of all considered metrics (plots for Pearson's R and ubRMSD are shown in Figure 7).

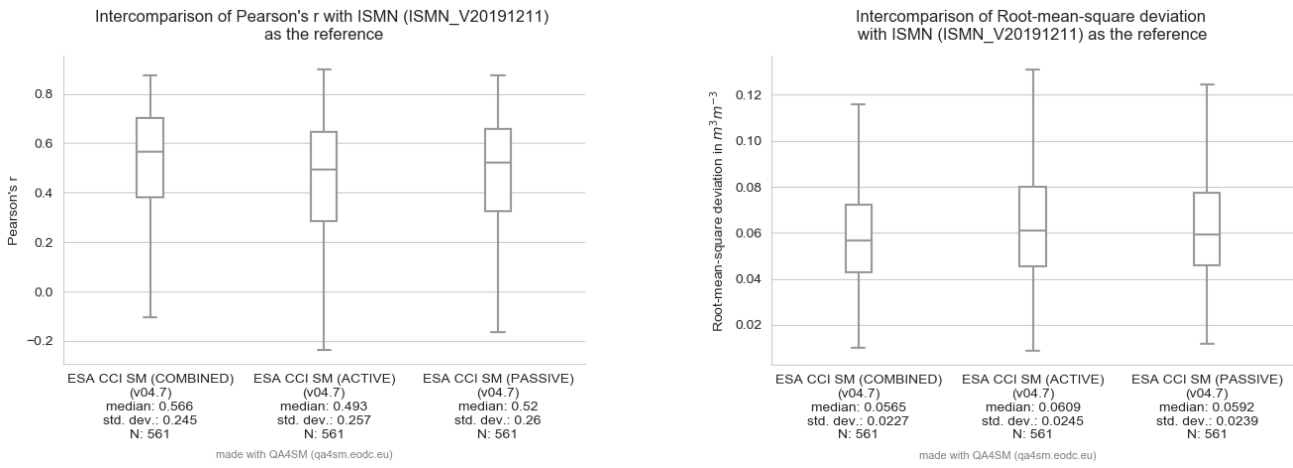


Figure 7 : Intercomparison of Pearson's R (left) and ubRMSD (right) for the ACTIVE, COMBINED and PASSIVE product in ESA CCI SM v04.7 with respect to ISMN reference data.

5.1.4 Validation with model reference data

The same analyses as described in section 5.1.3 are performed using GLDAS Noah as the reference data set. Also here virtually no differences between the two versions are found (compare Table 3, Figure 8 and Figure 9). GLDAS Noah Soil Moisture is scaled between 0 and 100 for the selected layer (whereas ISMN SM is between 0 and 1). This should be considered when comparing results for MSE and ubRMSD to those found with ISMN data.

| Metric | ACTIVE | | COMBINED | | PASSIVE | |
|-----------------------------|--------|-------|----------|-------|---------|-------|
| | v04.5 | v04.7 | v04.5 | v04.7 | v04.5 | v04.7 |
| MSE [kg/m ²] | 22 | 21.9 | 18.3 | 18.3 | 22.1 | 22.1 |
| Pearson's R [-] | 0.359 | 0.363 | 0.482 | 0.484 | 0.424 | 0.424 |
| Spearman's R [-] | 0.311 | 0.315 | 0.457 | 0.459 | 0.415 | 0.415 |
| ubRMSD [kg/m ²] | 4.69 | 4.68 | 4.28 | 4.27 | 4.7 | 4.7 |
| Kendall Tau [-] | 0.21 | 0.213 | 0.317 | 0.318 | 0.29 | 0.29 |

Table 3 : Median of all validation metrics derived from comparison to GLDAS Noah SM for ESA CCI SM v04.7 and v04.5 (ACTIVE, COMBINED and PASSIVE product).

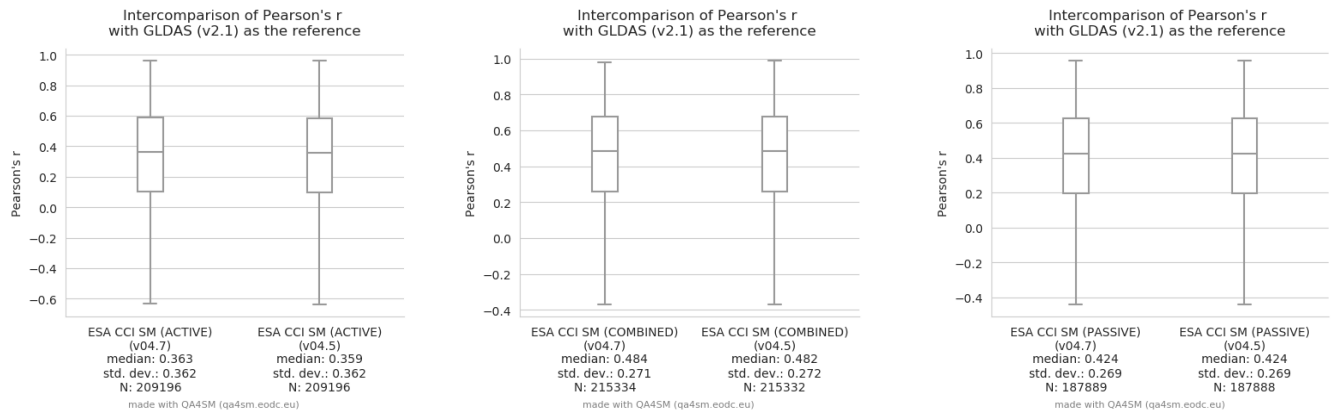


Figure 8 : Intercomparison of Pearson's R between ESA CCI SM v04.5 and v04.7 (ACTIVE, COMBINED, PASSIVE) with GLDAS Noah SM simulations as the reference

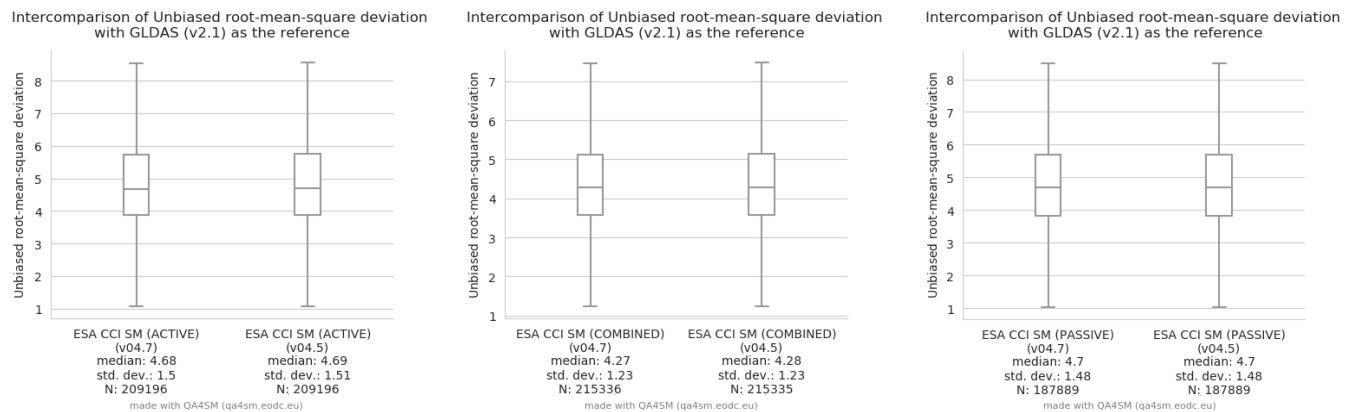


Figure 9 : Intercomparison of ubRMSD between ESA CCI SM v04.5 and v04.7 (ACTIVE, COMBINED, PASSIVE) with GLDAS Noah SM simulations as the reference

5.1.5 Summary

- The data set was successfully tested for completeness. Changes in the temporal coverage are either due to the performed temporal extension or vary slightly due to changes in the flagging of input data products.
- Comparison to ISMN data showed no significant differences from the previous version. In-depth comparison (e.g. in terms on landcover/climate) is provided in Section 0.
- Comparison to GLDAS Noah indicated no significant differences from the previous version. Validation with independent global reference data is presented in Section 0.



5.2 Comparison to in-situ observations from ISMN and global land reanalysis products (ETH Zürich)

5.2.1 Datasets and data processing

ESA CCI SM

To date various versions of the CCI soil moisture product are available. We use here v0.1, v02.2, v03.3, and the newest v04.7 release of the combined product derived from the collocated C-band scatterometer data set and the collocated multi-frequency radiometer data set. Additional intermediate releases are used for some of the analyses, these are v02.0, v02.1, v03.2, v04.2 and v04.4 (see Gruber et al. 2019 for an overview on the CCI SM product evolution). The spatial resolution of ESA CCI SM is 0.25° , with daily temporal resolution. Data is presented in m^3m^{-3} and represents soil moisture in the top few millimeters to centimeters of the soil (Kuria et al. 2007). The quality and availability of the data has increased over time, as the number of available satellites has increased (Dorigo et al. 2017; Dorigo et al. 2015; Dorigo et al. 2010).

ISMN

In-situ soil moisture measurements are obtained from the International Soil Moisture Network (ISMN). The ISMN database consists of measurements from various networks. If needed the data is transformed so that it is consistent in units ($\text{m}^3 \text{m}^{-3}$), then quality checked and flagged (Dorigo et al. 2011). The analyses are based on a full download from 14 April 2020. All data is aggregated to daily averages, considering only values with quality flag “G” (see <https://ismn.geo.tuwien.ac.at/en/data-access/quality-flags/>). This implicitly also masks soil temperatures $< 0^\circ\text{C}$.

Measurements from both the 5 cm and the 10 cm depths are considered since near-surface sensors appear to be more prone to errors (Mittelbach et al. 2012).

ERA5-Land, ERA-Interim/Land

To determine the influence of soil depth on soil moisture variability, we use ECMWF’s ERA5-Land reanalysis soil moisture (C3S 2019). ERA5-Land is available as a re-gridded 0.25° soil moisture product, corresponding to the ESA CCI SM resolution, and has global coverage. Here we use the top two soil layers, which represent 0-7 cm and 7-28 cm soil depths. Data is aggregated from the original hourly temporal resolution to daily averages. Moreover, the forerunner of ERA5-Land, ERA-Interim/Land (Balsamo et al. 2015; Dee et al. 2011) is used for comparison and as previous reanalysis benchmark in some of the analyses.

Data processing

We consider ISMN soil moisture measurements that have at least one year of data (i.e., 365 days with valid data) and focus the main analyses on the US, Europe, Africa and Australia as well as the time period 1991-2010, see Figure 10. This selection results in 334 individual soil moisture time series from 19 different networks. Soil moisture time series from the grid cells in which the stations fall are extracted from ESA CCI SM, ERA5-Land and ERA-Interim/Land for this comparison. The timeseries of the gridded products are scaled to the respective in-situ time series using a CDF matching approach.

Moreover, an extended time period up to 2019 is used for the evaluation of the product evolution over time (see Section **Error! Reference source not found.**). This, depending on the temporal subset under investigation, considers the extended set of currently available ISMN data with over 500 stations (cf. Section **Error! Reference source not found.**).

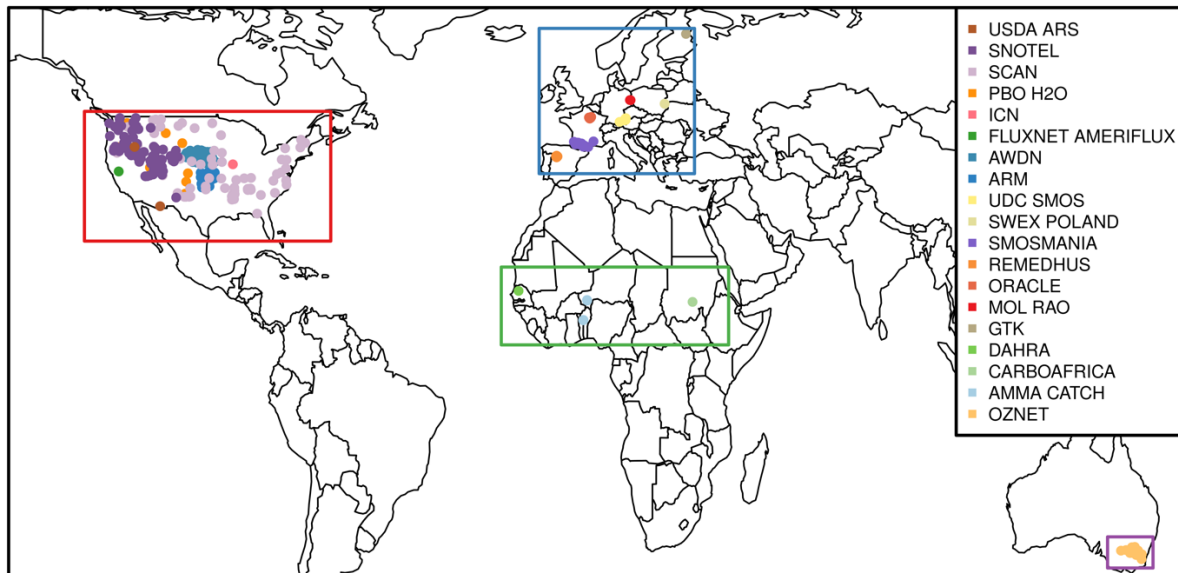


Figure 10: Overview of the spatial coverage of the stations considered in this study, rectangles indicate the four focus areas of the comparison, i.e., the United States (US, red), Europe (EU, blue), Africa (AF, green), and Australia (AUS, purple). Stations are color coded by network, see Figure 11 for the legend.

Comparisons of the products

In this study, we focus on the evaluation of ESA CCI SM v04.7 and compare it to its forerunners v0.1, v02.2, and v03.3, as well as to ERA5-Land and ERA-Interim/Land layer 1 and layer 2 soil moisture. Additional intermediate ESA CCI SM releases are used for some of the analyses, these are v02.0, v02.1, v03.2, v04.2 and v04.4. All considered data sets have a different temporal coverage, and we account for this by masking for common data availability and constraining our investigation to the period 1991-2010, see Figure 11.

To account for the different units and dynamic ranges of the products, and to remove systematic differences between the products, the ESA CCI SM, ERA5-Land and ERA-Interim/Land soil moisture time series are linearly scaled with respect to the mean and standard deviation of the in-situ time series (Brocca et al. 2010). Then, the long-term inter-annual anomalies are calculated based on subtracting the long-term mean using a 11-day window.

Agreement between in-situ data and ESA CCI SM, ERA5-Land and ERA-Interim/Land is determined by the Pearson correlation and by the unbiased root mean square difference (*ubRMSD*) between the in-situ time series and the corresponding time series from the gridded product. Note that because data availability varies among locations, the time period (and amount of data) used to calculate the statistical metrics may differ between locations. Also, most of the available in-situ data is from the US, so a general global conclusion cannot be

made. All analyses are performed on mean daily soil moisture, and results are shown for both the absolute scaled data, as well as the inter-annual anomalies.

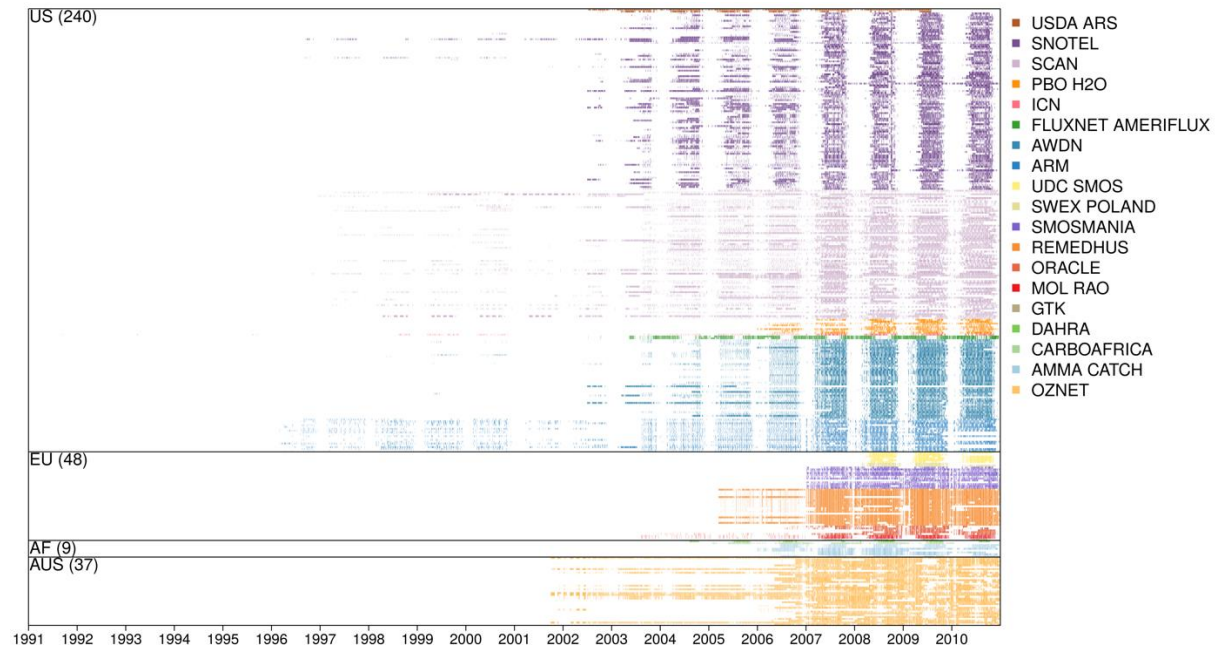


Figure 11: Overview of the temporal coverage of the stations considered in this study, after masking for common data availability, split per region. The number of stations per region is indicated in brackets.

5.2.2 General findings

We first focus on the correlations in the US only (Figure 12) and consider the first public version of the product (v0.1) and the three main product generations (as represented by the three major merging algorithms; see Gruber et al. 2019). Correlation is highest for the absolute values and drops considerably for the anomalies. We find that the spatial pattern of the ESA CCI SM correlations is rather scattered for the absolute values, and there are no clear areas in which the product agrees either very well or very poorly with in-situ soil moisture. Also, no pronounced difference in performance can be found between networks (not shown). For the anomalies, the ESA CCI SM correlations appear lower in the north-eastern of the region, which is likely related to complex topography. This is not the case for ERA5-Land layer 1.

There is a slight increase in correlation for each subsequent ESA CCI SM release, most notable when comparing v0.1 to v04.7. ERA5-Land layer 1 shows better agreement with in-situ soil moisture than ESA CCI SM, for both absolute values and anomalies.

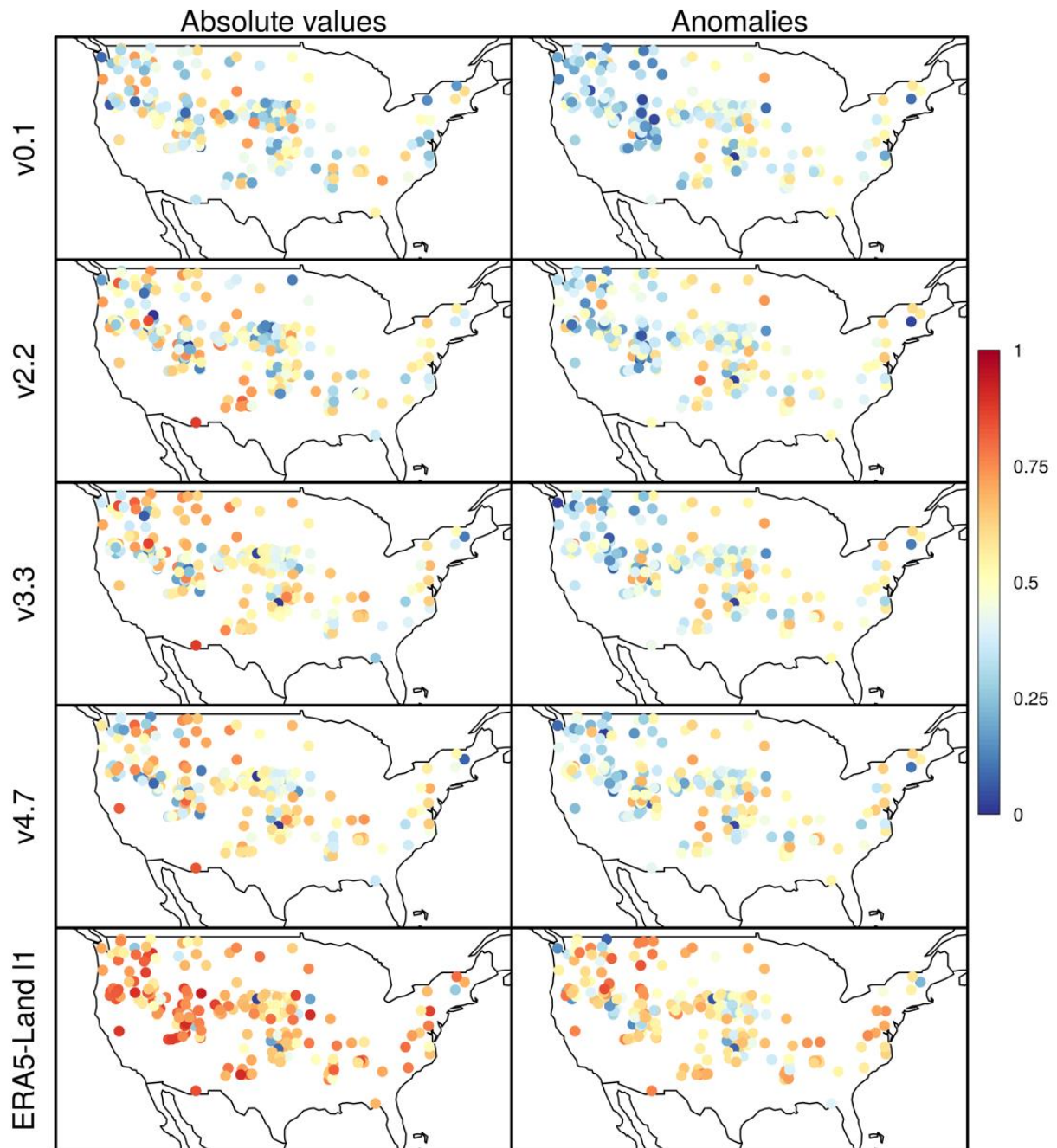


Figure 12: Correlation between in-situ soil moisture and ESA CCI SM for versions v0.1, v02.2, v03.3, and v04.7, as well as ERA5-Land soil moisture layer 1 (ERA5-Land I1, 0-7 cm), for absolute soil moisture (left) and the anomalies (right).

On the global scale (and for different climate zones), the correlations and ubRMSDs also indicate better agreement of ERA-Interim/Land and in particular of ERA5-Land with the in-situ data compared to the different ESA CCI SM releases (Figure 13 and Figure 14). The skill of ESA CCI SM appears to be slightly better for arid climate zones, both for absolute values and anomalies. A slight increasing tendency in the skill is again visible for the subsequent ESA CCI SM releases.

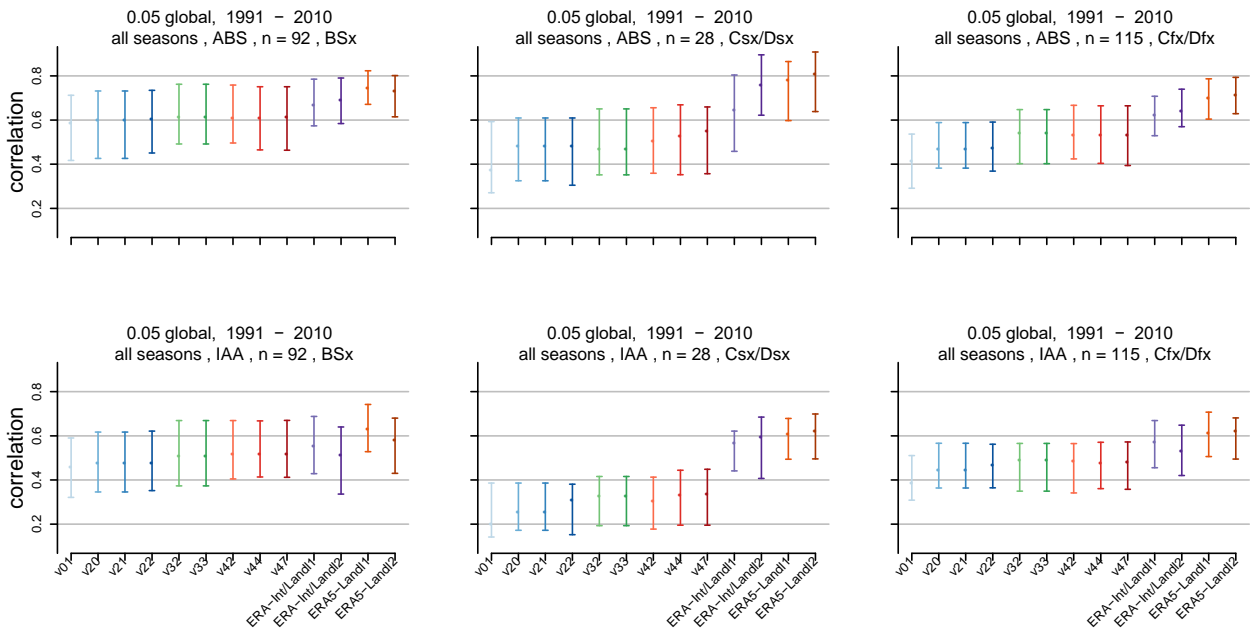


Figure 13: Correlation of the gridded soil moisture products as compared to in-situ station observations (5 cm depth) for three combinations of Köppen-Geiger classes (BSx - arid, Csx/Dsx - temperate/continental summer dry, Cfx/Dfx - temperate/continental without dry season). (Top row) Absolute values of soil moisture (ABS); (bottom row) inter-annual anomalies (IAA). Shown is the median and IQR of the correlations, n denotes the number of stations underlying the distributions.

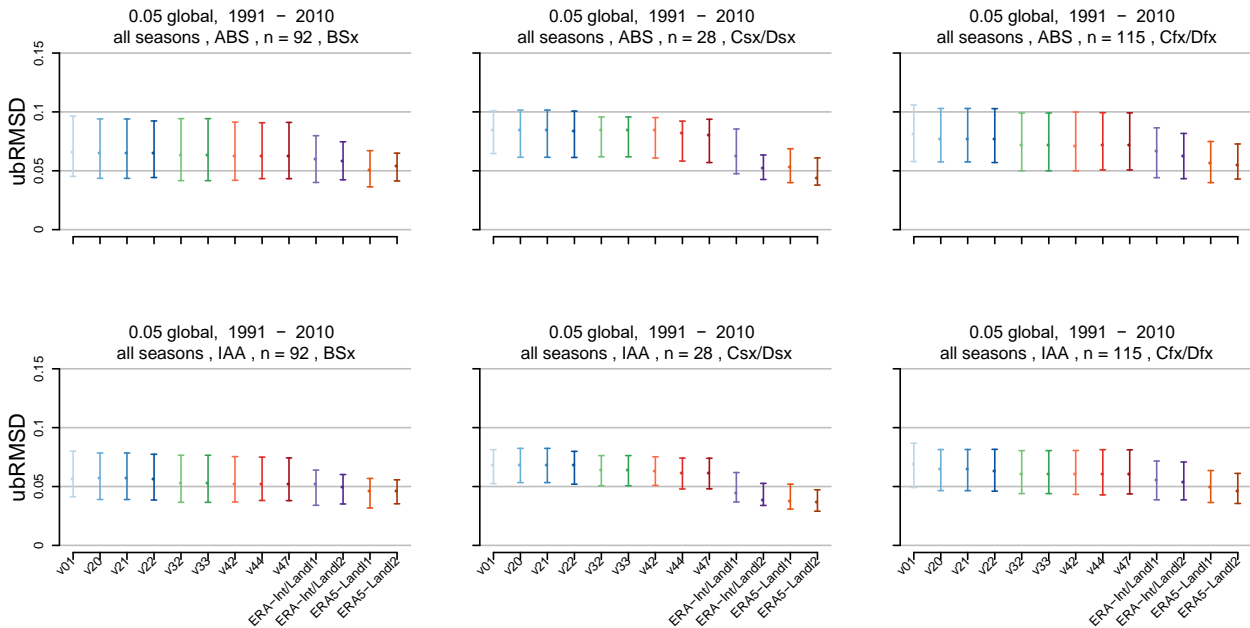


Figure 14: As Figure 13, but showing ubRMSD.

5.2.3 The influence of measuring depth

ESA CCI SM represents soil moisture in only the top few millimeters to centimeters of the soil (Dorigo et al. 2012; Dorigo et al. 2017). To determine the influence of measuring depth on the correlation we differentiate between measurements at 5 and 10 cm depth, see Figure 15. As noted above, the near-surface measurements may be more prone to errors (Mittelbach et al. 2012). Considering also the 10 cm measurements increases the robustness of the comparisons and may help to detect systematic degradations of the 5 cm sensors. For each product, we distinguish between three different regions (US, EU, and AUS) and show the results for the absolute values (top) as well as the anomalies (bottom). Circles denote correlations with in-situ measurements taken at 5 cm depth, and triangles at 10 cm depth.

ESA CCI SM: For the US and Europe, there is a large spread in the derived correlations, likely due to the large spread in climate conditions that the stations are located in. For Australia, the spread is much smaller, there are far fewer stations here and they are all located in the south-eastern part of the continent. For the US, the absolute values show correlations for the ESA CCI SM releases ranging between 0.1 to over 0.8 for the comparison with the 5 cm in-situ measurements, and between 0.1 to over 0.6 for the 10 cm measurements, with the median correlation for the shallower 5 cm in-situ measurements being consistently higher. For Europe, the correlations are higher with a median value around 0.6 for 5 cm depth for ESA CCI SM v0.1, and over 0.7 for v04.7. Again, the correlation with in-situ measurements at 10 cm depth is lower, though there are also less measurements available at this depth. The overall highest correlations are found in Australia, with up to 0.8 for the median. Again, the correlations are lower for 10 cm depth.

For the anomalies, the distinction between the 5 cm and the 10 cm correlations appears less pronounced, in particular in the US (where v0.1 even shows a reversed behavior, i.e., slightly higher 10 cm median correlation).

ERA5-Land: Consistent with ESA CCI SM, absolute values of ERA5-Land layer 1 (I1) and layer 2 (I2) show higher correlations with in-situ measurements at 5 cm depth than at 10 cm depth for the US and Europe. For Australia, the correlation is less dependent of the measuring depth, both for absolute values and the anomalies. For ERA5-Land I2, correlation with measurements taken at 10 cm are even slightly higher. For the anomalies, the results are comparable, though here the median correlation for 10 cm is also higher over Europe for ERA5-Land I2. The range of the correlations is similar to ESA CCI SM but goes up to over 0.9 for the absolute values. The median value is around 0.7, thus slightly higher than that of ESA CCI SM which is around 0.6 for v04.7.

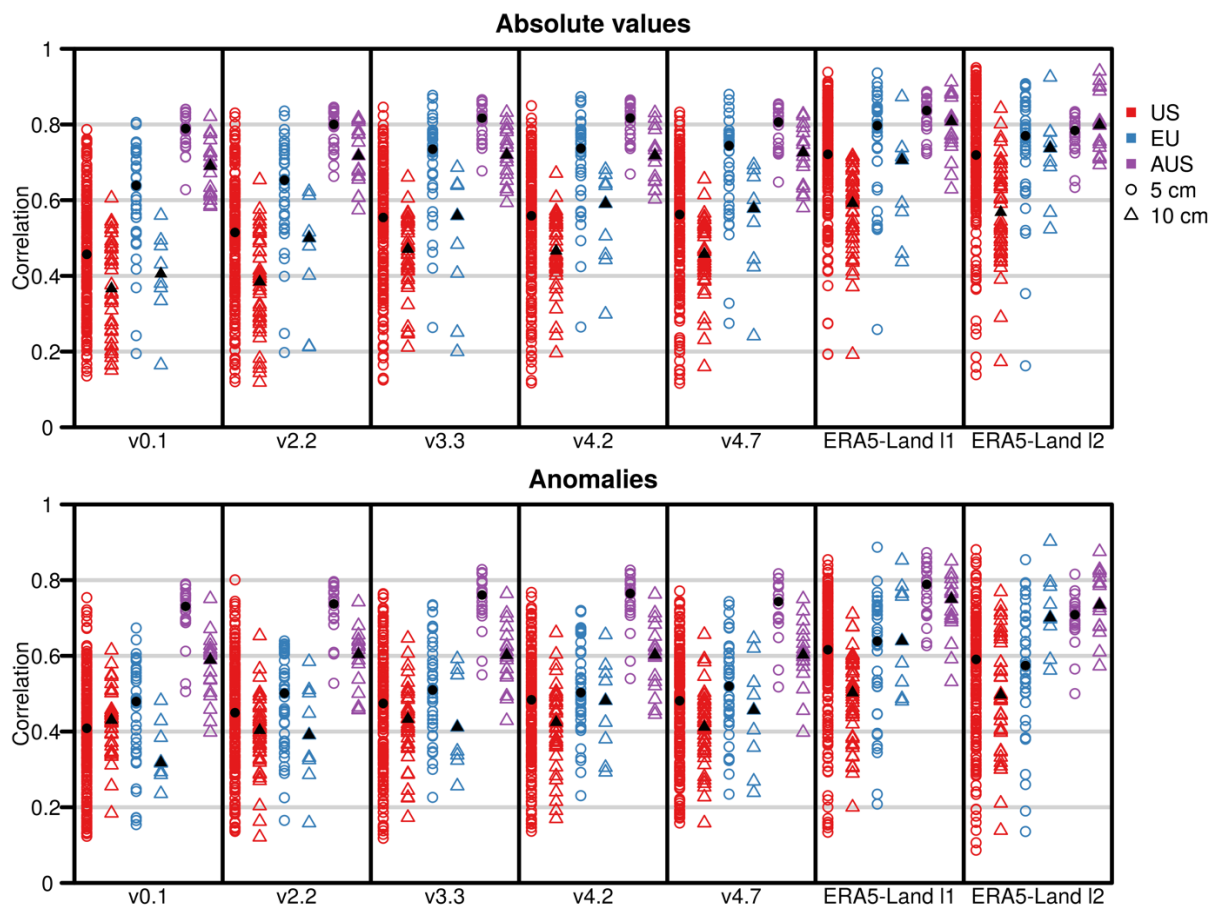


Figure 15: Correlation between in-situ measurements for ESA CCI SM v0.1, v02.2, v03.3, v04.2, and v04.7, as well as ERA5-Land soil moisture layer 1 and 2 for the absolute soil moisture values (top) and the anomalies (bottom). For each product, we distinguish between 3 regions US, EU, and AUS (red, blue and purple, AF has insufficient data coverage), and the correlation at 5 cm depth (circles) and 10 cm depth (triangles). The same number of stations is taken into account for the individual distributions of the top and bottom panels. The black circles/triangles represent the respective median values.

5.2.4 The influence of land cover

Figure 16 shows the correlations for ESA CCI SM v0.1, v02.2, v03.3, and v04.7, as well as ERA5-Land layer 1 over the US for absolute values and their inter-annual anomalies, differentiating between grassland (orange) and forest (green) sites (based on the land-cover information of



the ISMN stations). As above, correlations for the anomalies are lower compared to the absolute values for all products. For all versions of ESA CCI SM, there is a notably higher correlation for grassland sites than for forest sites, both for the absolute values as well as the anomalies. This is related to the reduced retrieval quality over more densely vegetated areas. For ERA5-Land, such a distinction in the skill between the two land cover types is not visible.

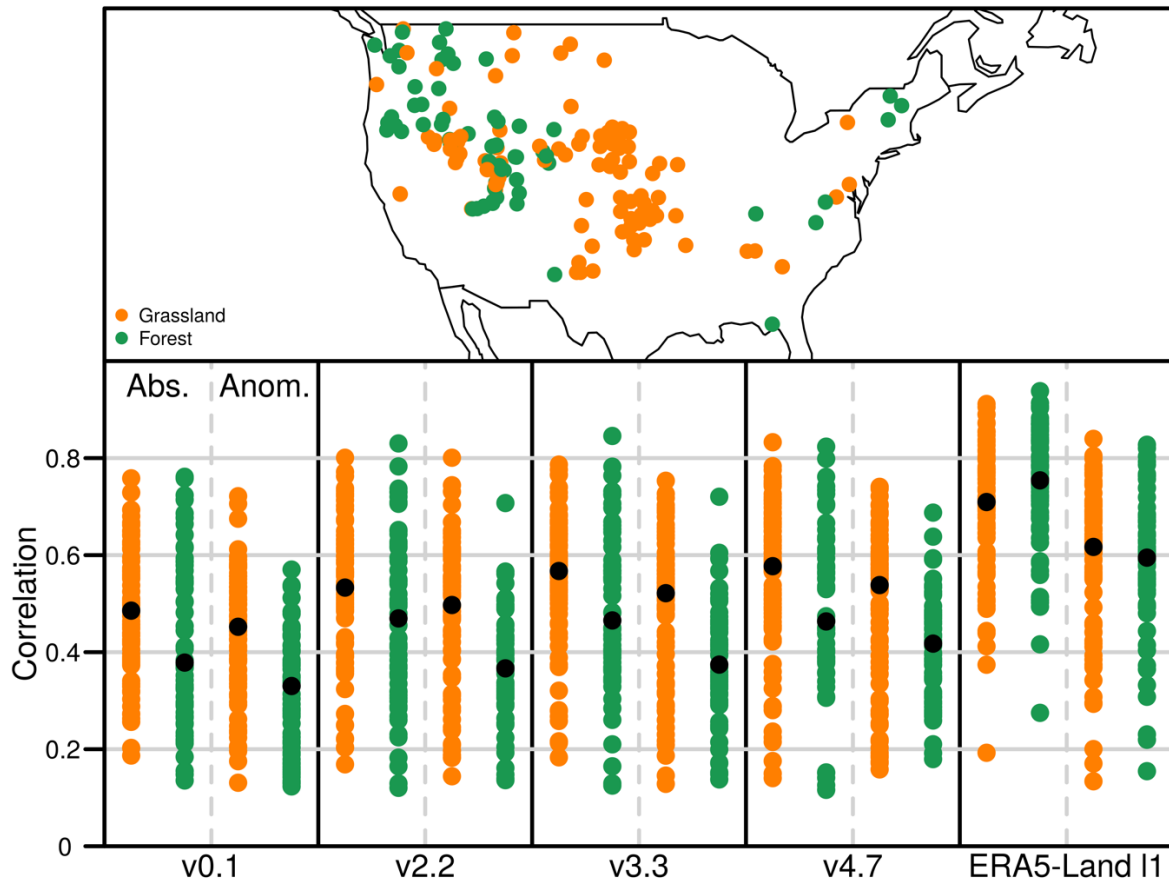


Figure 16: Correlation between in-situ measurements at 5 cm depth and ESA CCI SM v0.1, v02.2, v03.3, and v04.7, as well as ERA5-Land soil moisture layer 1, differentiating between grassland (orange) and forest (green) sites for absolute soil moisture values and anomalies. Black dot denotes the median value.

5.2.5 Temporal subsets and product evolution

Figure 17 shows the (significantly positive, $p < 0.05$) correlations of the different ESA CCI SM releases, as well as ERA5-Land and ERA-Interim/Land layer 1 compared to in-situ stations (extended set of stations, see Section 5.2.1) in the US for different temporal subsets (i.e., 1997-2000, 2001-2004, 2005-2008, 2009-2012, and 2013-2016, as well as 1997 up to the end of the individual time series). The overall correlations for ESA CCI SM appear higher in the earliest period, with a drop during 2001-2004 and subsequent increase towards later periods. This behaviour is in particular visible for summer (not shown). The correlations of ERA5-Land are stable over time, while ERA-Interim/Land also displays a drop in 2001-2004.

The ESA CCI SM releases show a general increase in performance with data releases, pointing to the increasing maturity of the product.

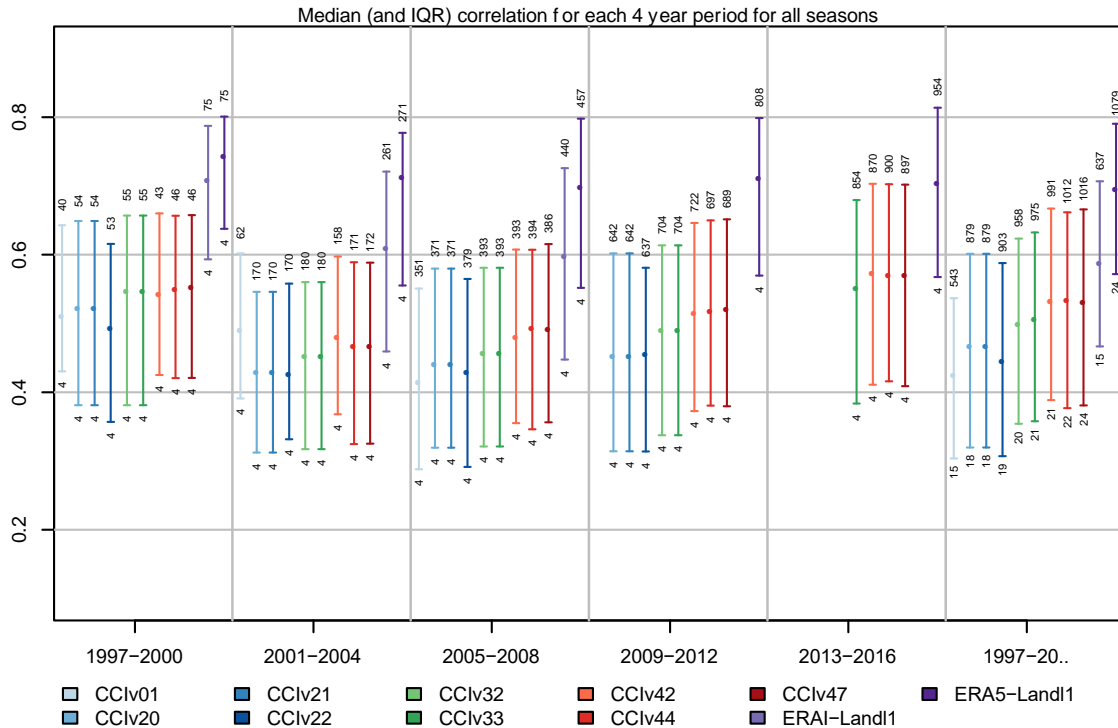


Figure 17: Correlation of the gridded soil moisture products as compared to in-situ station observations in 5 and 10 cm depth for the full year for the US. Subdivided in consecutive 4-year periods (1997-2000, 2001-2004, 2005-2008, 2009-2012, and 2013-2016) as well as for the longest period data is available (1997-20.., end date would e.g. be 2010 for CCI v0.1, but is 2016 for e.g. CCI v4.1). Note that in this case, data is not masked for common data availability. Whiskers show the median and the IQR. Above indicated the number of stations correlations were calculated for that comply to the following criteria: at least 10% of the timeseries is not NA, p -value < 0.05 , and the calculated correlation is positive. And below indicated the number of years considered.

5.2.6 Summary

- Spatially scattered pattern in correlations, no clear areas in which the ESA CCI SM products agree either very well or very poorly with in-situ soil moisture. Though, highest correlations are found in Australia, which corresponds to overall higher correlations and lower ubRMSDs in arid climate.
- ESA CCI SM clearly shows a higher correlation with in-situ measurements at 5 cm depth than at 10 cm depth. For ERA5-Land this distinction is less clear.
- ESA CCI SM clearly shows higher correlations with in-situ measurements over grassland sites than over forest sites. For ERA5-Land this difference is not visible.

- In particular the newly released ERA5-Land reanalysis soil moisture on the average shows better agreement with the in-situ data compared to the ESA CCI SM product. However, the ESA CCI SM show a general increase in skill with subsequent data releases, pointing to the increasing maturity of the remote sensing product.

6 Validation activities towards future algorithm development

6.1 Evaluation of different SMOS and SMAP algorithms with respect to GLDAS (CESBIO)

One of the mayor goals of future versions of the ESA CCI SM dataset is to remove the dependence on the model that it is used as reference for the rescaling of different remote sensing time series: the Global Land Data Assimilation System (GLDAS) Noah model. Taking into account the results of the ESA Passive Microwave Soil Moisture Data Fusion project (van der Schalie et al. 2016b) L-band data from the two sensors that have been specifically designed to measure soil moisture (ESA Soil Moisture and Ocean Salinity –SMOS- and NASA Soil Moisture Active Passive - SMAP) could be used as reference to rescale the time series of the other sensors used in the ESA CCI SM. Several soil moisture datasets obtained from SMOS and SMAP observations are available. It is therefore pertinent to compare those datasets respect to GLDAS in order to evaluate the possible impacts of replacing the GLDAS model by a SMOS or SMAP dataset.

6.1.1 Datasets and data processing

The SMOS soil moisture data sets used in this study are the CATDS Level 3 (Al Bitar et al. 2017) version 300, the ESA Near-Real-Time version 2 (Rodriguez-Fernandez et al. 2017), the INRA-CESBIO (Fernandez-Moran et al. 2017) version 1 and the LPRM version 6 dataset used by the ESA CCI project (Van der Schalie et al. 2016a). The SMAP datasets used are the Level 2 product and the LPRM version 6 dataset used by the ESA CCI project. The GLDAS Noah model version 2.1 (Rodell et al. 2004) was used to compare the remote sensing datasets.

The two LPRM datasets and the GLDAS model were provided by TU Wien in the ESA CCI SM spatial grid. The other products were spatially interpolated from their original grids to the ESA CCI SM grid.

6.1.2 Evaluation with respect to in-situ measurements

Figure 18 shows the results of the evaluation of the different products with respect to in-situ measurements for the stations of the SCAN and USCRN networks retrieved from the International Soil Moisture Network (Dorigo et al. 2011). SMOS Level 3 data show the higher standard deviation and lower correlation with respect to the in-situ measurements. SMOS LPRM, IC and NRT show similar results for SCAN (with a slightly higher median correlation for the NRT) and close to those of GLDAS. The correlation of SMAP Level 2 with respect to in-situ is lower than that of SMOS products but it is similar to that of SMOS for SMAP LPRM at USCRN



stations and even somewhat higher at SCAN stations. GLDAS and SMAP show a positive bias with respect to the in-situ measurements while SMOS products show a negative bias.

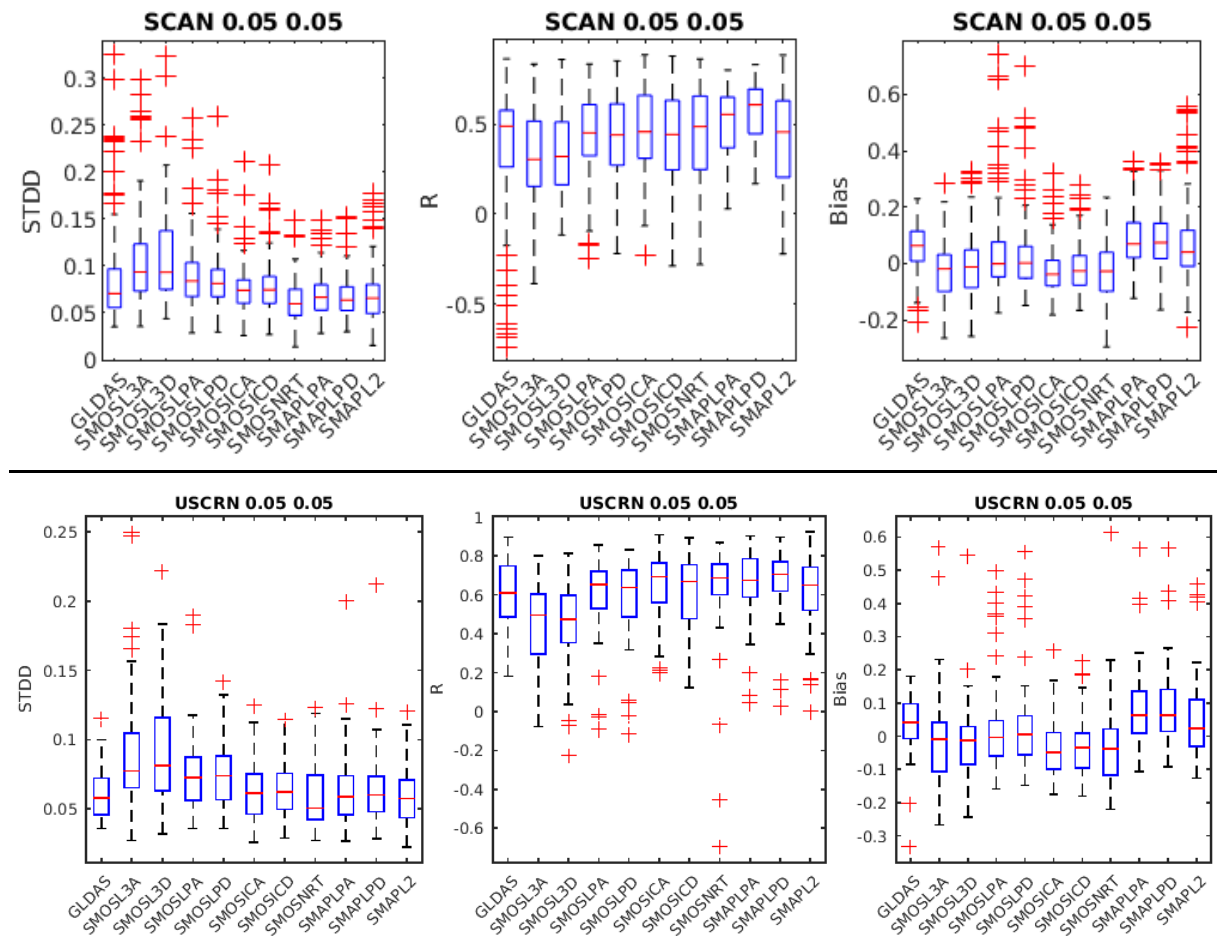


Figure 18: Box plots for the standard deviation of the difference (STDD, left), the Pearson correlation (R, center) and the bias (remote sensing or model minus in-situ, right) with respect to in-situ measurements from the SCAN (upper panels) and USCRN (lower panels) networks. The red line is the median of the distribution and the blue box represent the data within the 25th and the 75th percentile of the sample data (q_1 and q_3 , respectively). The whiskers extend from $q_3 + 1.5 \times (q_3 - q_1)$ to $q_1 - 1.5 \times (q_3 - q_1)$. Samples outside this range are considered as outliers (red crosses). The datasets that are evaluated are GLDAS, SMOS L3 for ascending and descending orbits (SMOSL3 A and D), SMOS LPRM for ascending and descending orbits (SMOSLP A and D), SMOS Near-Real-Time (SMOSNRT), SMOS IC (SMOSIC A and D), SMAP Level 2 (SMAPL2) and SMAP LPRM for ascending and descending orbits (SMAPLP A and D).

6.1.3 Comparison of the temporal dynamics with respect to GLDAS

In order to evaluate the temporal dynamics of the different datasets, Figure 19 shows Pearson correlation maps of the SMAP and SMOS products with respect to GLDAS. All of the SMAP and SMOS products show negative correlation values for high latitudes and in the dense equatorial forest. The SMOS LPRM dataset also shows negative correlations in the areas surrounding the blank regions where radio frequency interferences are the most likely. However, this is not present in the correlation maps for other SMOS products.

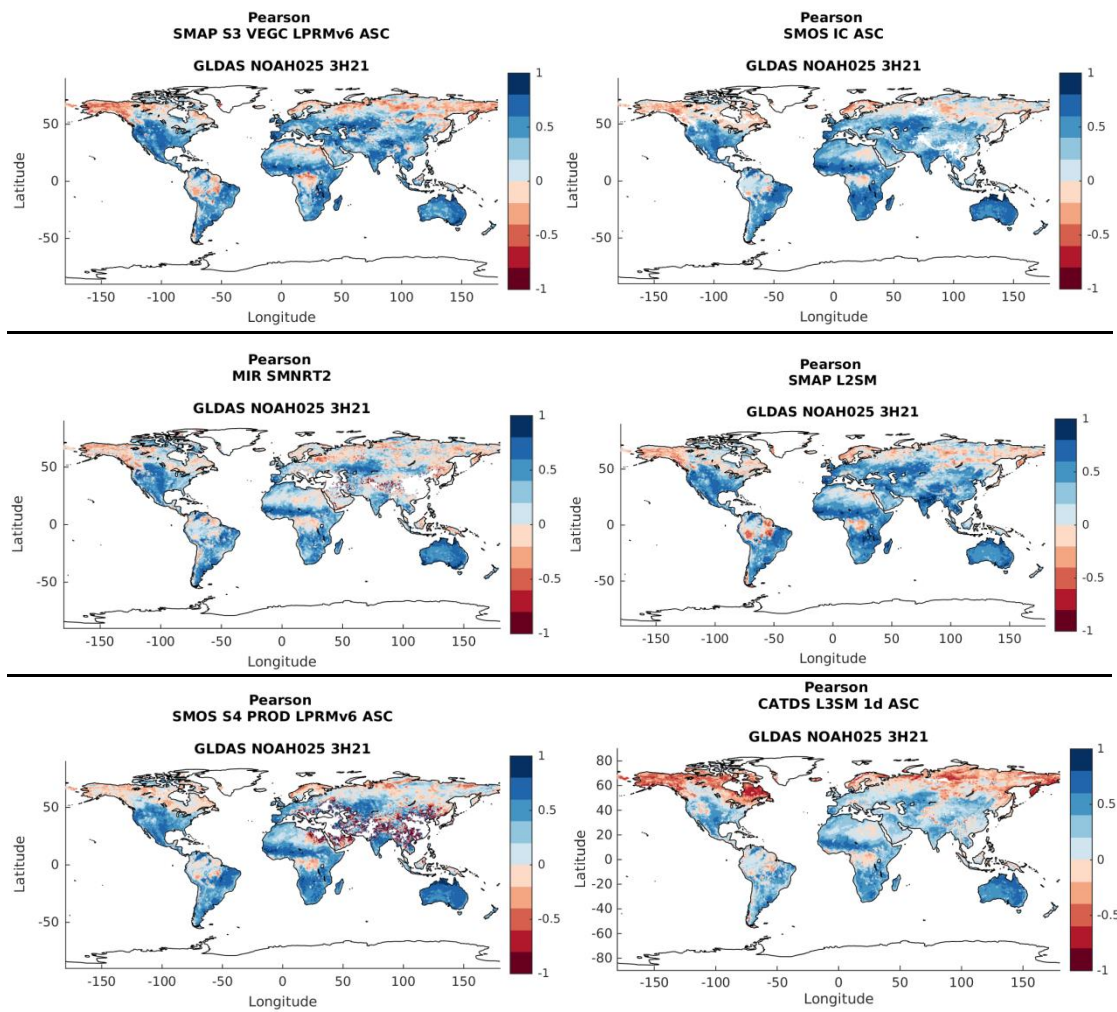


Figure 19: Maps of the Pearson correlation with respect to GLDAS of the SMAP LPRM and SMOS CATDS L3, LPRM and IC for ascending orbits, the SMOS NRT and the SMAP Level 2 products.

6.1.4 Comparison of the Cumulative Distribution Functions

Currently, the rescaling of active and passive sensors time series is done using the GLDAS model by matching the cumulative distribution functions (CDFs) of the different remote sensing time series to that of GLDAS (Liu et al. 2011). The CDF of a variable x , evaluated at x_0 , is the probability that x will take a value less than or equal to x_0 . Here, the CDFs have been computed dividing the 0-1 m^3/m^3 soil moisture interval in 30 bins, which implies a bin width of $0.033 \text{ m}^3/\text{m}^3$, comparable to the targeted uncertainty of most remote sensing soil moisture products of $0.04 \text{ m}^3/\text{m}^3$. This bin width allows a good sampling of the high slope region of the CDF.

GLDAS time series have been temporally interpolated to the acquisition time of each remote sensing product and sampled so that the GLDAS time series contains the same number of points of the remote sensing time series. Figure 21 shows examples of the CDFs at one position

in North America. The impact of the temporal interpolation and sampling of GLDAS is low as the different GLDAS CDFs shown in the different panels of Figure 21 are very similar.

In order to summarize the differences of two CDFs and to visualize the spatial distribution of those differences, two methods were tested. In the first method, the CDF difference for the bin with larger difference in between the two products was computed for each node of the ESA CCI SM grid. In the second method, the difference of the CDF of the two products was computed for each of the 30 bins. The addition of the absolute values of those differences was computed and divided by 30. Only the results for the second approach are discussed here as it gives a more robust estimation of the overall differences of two CDFs than using just the difference for one single soil moisture bin.

Figure 20 shows maps of the four SMOS and two SMAP products that were compared. For those that are provided in ascending and descending orbits separately, only ascending orbits are shown. The regions where the differences are higher will be those where the impact of replacing GLDAS by a SMAP or SMOS product will be the most significant.

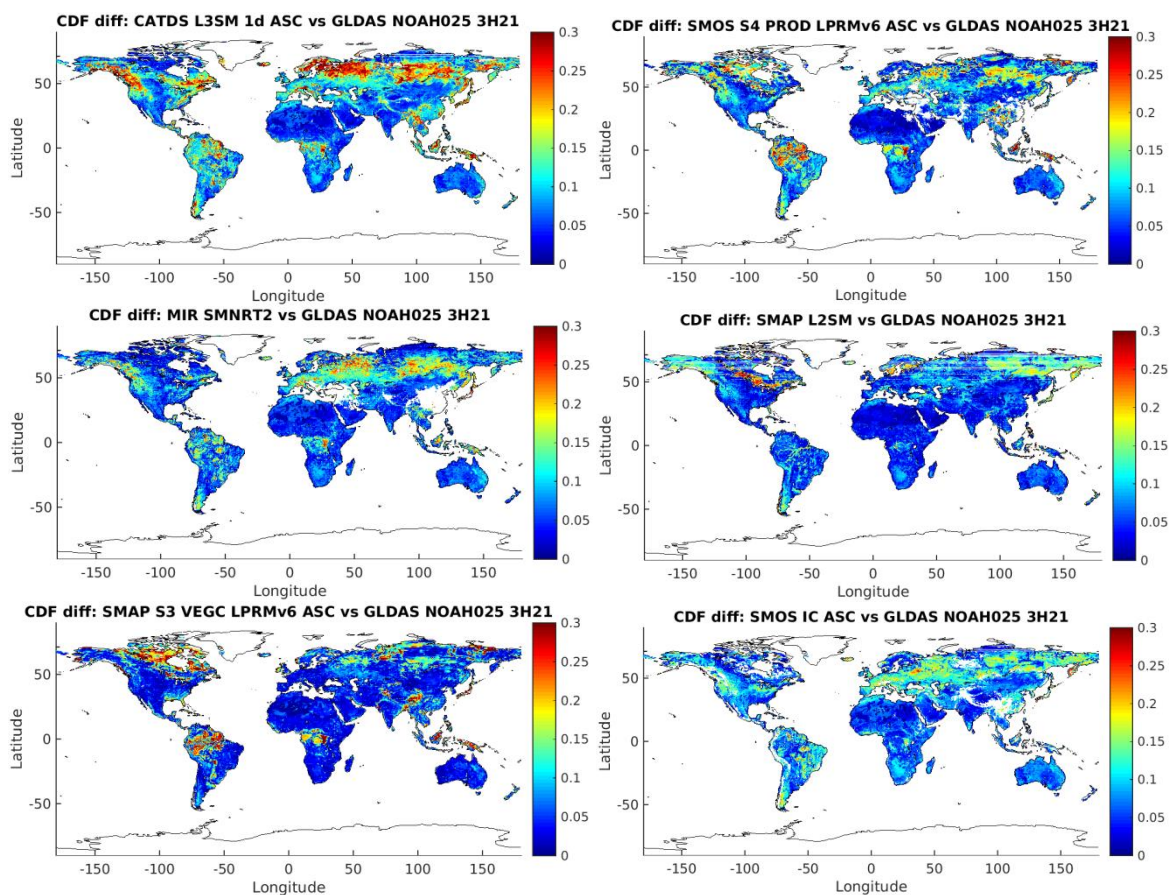


Figure 20: Maps of the sum of absolute differences of the CDFs of SMOS and SMAP products with respect to the GLDAS CDF computed in 30 bins.

Both LPRM products show strong differences in the CDF with respect to that of GLDAS in South America (Amazon and Orinoco basins) and in the north of Canada. Those strong CDF



differences in these regions are not seen in the other SMAP or SMOS products. The SMOS CATDS Level 3 product shows strong CDF differences with respect to GLDAS at latitudes of $\sim 60^\circ$ North. The CDF differences also increase in these regions for the SMOS NRT (MIR SMNRT2), LPRM and IC products.

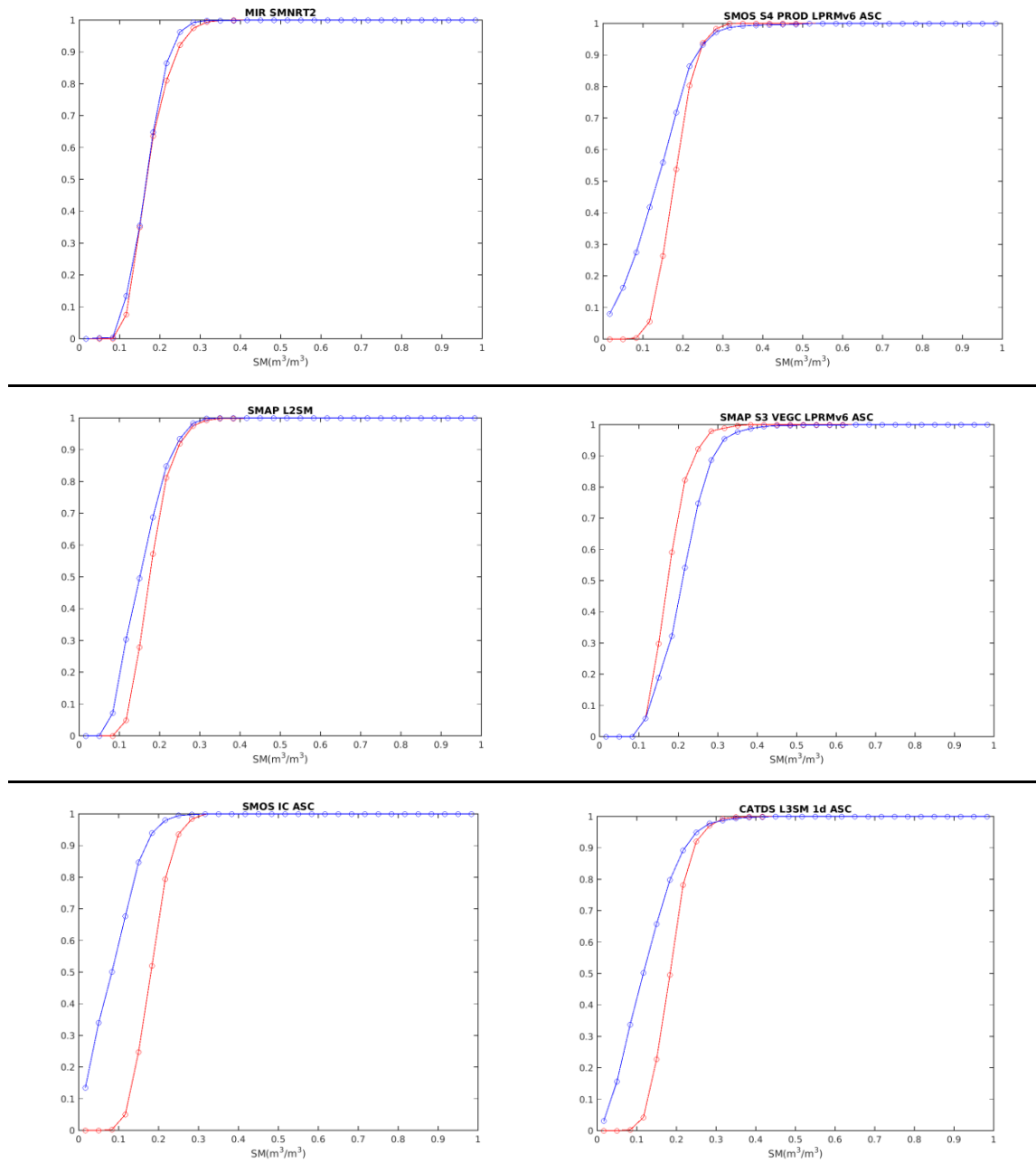


Figure 21: Blue circles and lines show the CDF for different SMOS and SMAP products while red circles and line shows the CDF for the GLDAS time series temporally interpolated at the acquisition times of each SMAP and SMOS products (for the closest grid point to longitude -100° and latitude 40°).

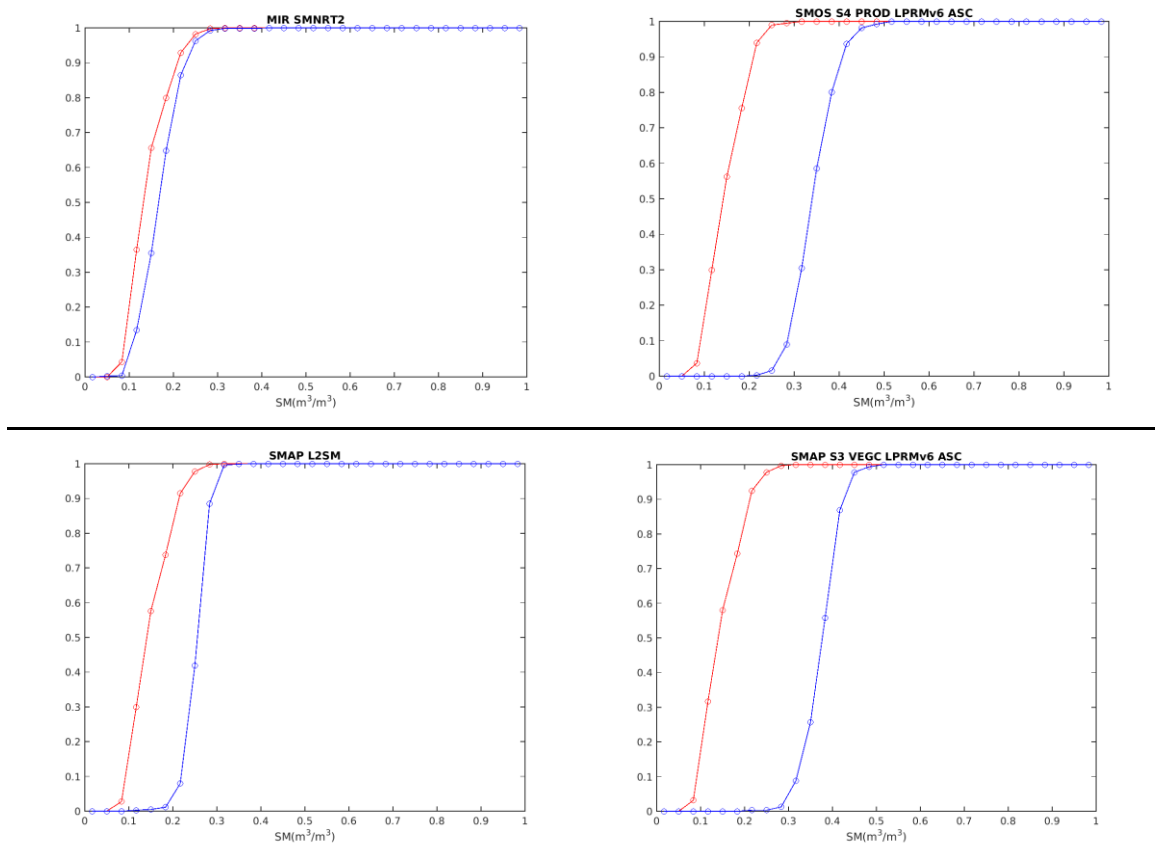


Figure 22: Blue circles and lines show the CDF for different SMOS and SMAP products while red circles and line shows the CDF for the GLDAS time series temporally interpolated at the acquisition times of each SMAP and SMOS products (for the closest grid point to longitude -100° and latitude 65°).

Figure 22 shows the CDFs at longitude -100° , latitude 65° , the differences with respect to GLDAS increase significantly for all products with respect to those shown in Figure 21 for longitude -100° , latitude 40° . Globally, except in the regions where the differences are strong, the overall agreement of SMAP and GLDAS CDFs is good with very low values for the CDF differences.

The possible impact of the length of the time series in the CDF computation was also studied. SMOS times series are available since 2010, while SMAP time series are available since 2015. The CDFs of the SMOS time series were also computed using data from 2015-2019 and were compared to GLDAS CDFs in the same way as the 2010-2019 time series. This was done for all the SMOS products. Figure 23 shows the CDF difference map and the CDF for one grid point for the SMOS IC ASC dataset. These plots can be compared to those in Figure 20 and Figure 21. There are actually no significant differences with respect to the results obtained using the full length of the SMOS time series. The same result was obtained for the other SMOS datasets.

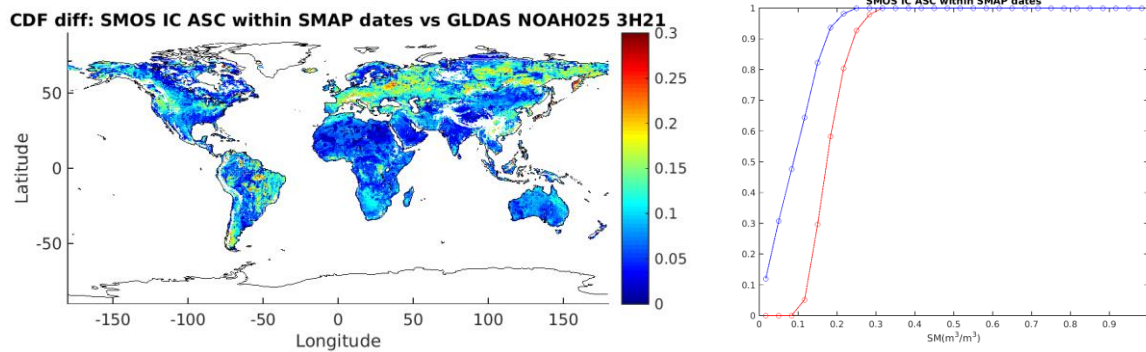


Figure 23: Left: map of the CDF differences from SMOS IC ASC and GLDAS computed SMOS data only with dates after the launch of SMAP. Right: Blue circles and lines show the CDF for the SMOS IC ASC product computed from the launch date of SMAP while red circles and line shows the CDF for the GLDAS time series temporally interpolated at the acquisition times of SMOS (for the closest grid point to longitude -100° and latitude 40°).

6.1.5 Summary

One of the major goals of the current phase of the project is to remove the dependence of the combined product on models. In particular, the GLDAS model, used as reference for the rescaling of the different time series, could be replaced by a remote sensing dataset from an L-band sensor (SMOS or SMAP). Following the Algorithm Development Plan, this is currently planned to take place in Version 7. To prepare future developments, it is necessary to evaluate different SMAP and SMOS products and to identify the regions where the CDFs differ the most with respect to GLDAS, as those are the regions where the impact of replacing GLDAS by a remote sensing dataset will be the most significant.

The evaluation of GLDAS and the different SMAP and SMOS products with respect to in-situ measurements give similar results except for the SMOS CATDS Level 3 dataset, which shows higher STDD and lower correlation R. The correlation maps also show the lowest values for the SMOS CATDS Level 3 product. Otherwise, these maps show that the SMOS and SMAP temporal dynamics are not in agreement with that of GLDAS in Northern latitudes and in the Equatorial forest. In addition to showing different temporal dynamics and low correlation, these regions are also those where the actual soil moisture distributions differ the most, as shown by the CDF differences maps.

This study allowed identifying the regions where the impacts of performing the rescaling of the different time series with respect to an L-band dataset will be the most significant. In contrast, it does not give a clear answer to the question of which of the L-band products could be the best suited to replace the model. However, it was shown that using only shorter time period for which SMAP is available does not affect significantly the CDF computation. Further studies would be needed to fully understand the impact of replacing GLDAS, in particular performing actual rescaling of other sensors such as AMSR-2.

7 Conclusions

Based on the various verification and validation activities described in this PVIR, the current ESA CCI SM v04.7 product is generally suitable for representing the spatio-temporal evolution of surface soil moisture (in particular, its temporal dynamics). The product shows a general increase in skill with subsequent data releases, which points to the increasing maturity of the ESA CCI SM product.

The skill of ESA CCI SM appears slightly better for arid climate. Moreover, previous validation activities further showed that the ESA CCI SM product suffers shortcomings at northern high latitudes (northward of 60°N, though improving from earlier products), over regions with complex topography and regions with dense vegetation, all areas well known to be difficult to monitor from remote sensing platforms.

Within the ESA CCI SM v04.7, the COMBINED product performs best in terms of all considered metrics, which clearly shows the benefit of merging active and passive remote sensing for global surface soil moisture.

One goal of current R&D within the ESA CCI SM project is to remove the dependency of the product from the land-surface model estimates of GLDAS, which is used as reference for the rescaling of remote sensing time series. As a possible alternative, L-band soil moisture from SMOS and SMAP could be used as a reference to rescale the time series of the other sensors. Evaluation of different SMOS and SMAP algorithms and GLDAS show mostly similar performance as compared to in-situ measurements. Furthermore, northern latitudes and equatorial forests show most pronounced disagreement between the SMOS and SMAP temporal dynamics and GLDAS. Thus, these regions will be most impacted by a possible switch of the rescaling procedure within ESA CCI SM to an L-band product.

Finally, the potential of data assimilation for adding value to the ESA CCI SM product has been noted in previous PVIRs, e.g., by providing soil moisture information at higher spatial resolution in the horizontal, and in the vertical (e.g., providing information on root zone soil moisture). This is especially relevant for regions where high quality precipitation data sets are lacking, here the ESA CCI SM product can provide valuable additional information of the state of the land surface. Various workshops and meetings within the ESA CCI for soil moisture have identified the importance of root zone soil moisture information for studies of the climate system, including the hydrological and carbon cycles.



8 Bibliography

Al Bitar, A., Mialon, A., Kerr, Y.H., Cabot, F., Richaume, P., Jacquette, E., Quesney, A., Mahmoodi, A., Tarot, S., Parrens, M., Al-Yaari, A., Pellarin, T., Rodriguez-Fernandez, N., & Wigneron, J.P. (2017). The global SMOS Level 3 daily soil moisture and brightness temperature maps. *Earth System Science Data*, *9*, 293-315

Balsamo, G., Albergel, C., Beljaars, A., Boussetta, S., Brun, E., Cloke, H., Dee, D., Dutra, E., Munoz-Sabater, J., Pappenberger, F., de Rosnay, P., Stockdale, T., & Vitart, F. (2015). ERA-Interim/Land: a global land surface reanalysis data set. *Hydrology and Earth System Sciences*, *19*, 389-407

Brocca, L., Melone, F., Moramarco, T., & Morbidelli, R. (2010). Spatial-temporal variability of soil moisture and its estimation across scales. *Water Resources Research*, *46*

C3S (2019). C3S ERA5-Land reanalysis. Copernicus Climate Change Service. In. <https://cds.climate.copernicus.eu/cdsapp#!/home>

Dee, D.P., Uppala, S.M., Simmons, A.J., Berrisford, P., Poli, P., Kobayashi, S., Andrae, U., Balmaseda, M.A., Balsamo, G., Bauer, P., Bechtold, P., Beljaars, A.C.M., van de Berg, L., Bidlot, J., Bormann, N., Delsol, C., Dragani, R., Fuentes, M., Geer, A.J., Haimberger, L., Healy, S.B., Hersbach, H., Holm, E.V., Isaksen, L., Kallberg, P., Kohler, M., Matricardi, M., McNally, A.P., Monge-Sanz, B.M., Morcrette, J.J., Park, B.K., Peubey, C., de Rosnay, P., Tavolato, C., Thepaut, J.N., & Vitart, F. (2011). The ERA-Interim reanalysis: configuration and performance of the data assimilation system. *Quarterly Journal of the Royal Meteorological Society*, *137*, 553-597

Dorigo, W., de Jeu, R., Chung, D., Parinussa, R., Liu, Y., Wagner, W., & Fernandez-Prieto, D. (2012). Evaluating global trends (1988-2010) in harmonized multi-satellite surface soil moisture. *Geophysical Research Letters*, *39*

Dorigo, W., Wagner, W., Albergel, C., Albrecht, F., Balsamo, G., Brocca, L., Chung, D., Ertl, M., Forkel, M., Gruber, A., Haas, E., Hamer, P.D., Hirschi, M., Ikonen, J., de Jeu, R., Kidd, R., Lahoz, W., Liu, Y.Y., Miralles, D., Mistelbauer, T., Nicolai-Shaw, N., Parinussa, R., Pratola, C., Reimer, C., van der Schalie, R., Seneviratne, S.I., Smolander, T., & Lecomte, P. (2017). ESA CCI Soil Moisture for improved Earth system understanding: State-of-the art and future directions. *Remote Sensing of Environment*, *203*, 185-215

Dorigo, W.A., Gruber, A., De Jeu, R.A.M., Wagner, W., Stacke, T., Loew, A., Albergel, C., Brocca, L., Chung, D., Parinussa, R.M., & Kidd, R. (2015). Evaluation of the ESA CCI soil moisture product using ground-based observations. *Remote Sensing of Environment*, *162*, 380-395

Dorigo, W.A., Scipal, K., Parinussa, R.M., Liu, Y.Y., Wagner, W., de Jeu, R.A.M., & Naeimi, V. (2010). Error characterisation of global active and passive microwave soil moisture datasets. *Hydrology and Earth System Sciences*, *14*, 2605-2616

Dorigo, W.A., Wagner, W., Hohensinn, R., Hahn, S., Paulik, C., Xaver, A., Gruber, A., Drusch, M., Mecklenburg, S., van Oevelen, P., Robock, A., & Jackson, T. (2011). The International Soil



Moisture Network: a data hosting facility for global in situ soil moisture measurements. *Hydrology and Earth System Sciences*, 15, 1675-1698

Fernandez-Moran, R., Al-Yaari, A., Mialon, A., Mahmoodi, A., Al Bitar, A., De Lannoy, G., Rodriguez-Fernandez, N., Lopez-Baeza, E., Kerr, Y., & Wigneron, J.P. (2017). SMOS-IC: An Alternative SMOS Soil Moisture and Vegetation Optical Depth Product. *Remote Sensing*, 9

Gruber, A., Scanlon, T., van der Schalie, R., Wagner, W., & Dorigo, W. (2019). Evolution of the ESA CCI Soil Moisture climate data records and their underlying merging methodology. *Earth System Science Data*, 11, 717-739

Kuria, D.N., Koike, T., Lu, H., Tsutsui, H., & Graf, T. (2007). Field-supported verification and improvement of a passive microwave surface emission model for rough, bare, and wet soil surfaces by incorporating shadowing effects. *Ieee Transactions on Geoscience and Remote Sensing*, 45, 1207-1216

Mittelbach, H., Lehner, I., & Seneviratne, S.I. (2012). Comparison of four soil moisture sensor types under field conditions in Switzerland. *Journal of Hydrology*, 430, 39-49

Rodell, M., Houser, P.R., Jambor, U., Gottschalck, J., Mitchell, K., Meng, C.J., Arsenault, K., Cosgrove, B., Radakovich, J., Bosilovich, M., Entin, J.K., Walker, J.P., Lohmann, D., & Toll, D. (2004). The global land data assimilation system. *Bulletin of the American Meteorological Society*, 85, 381-394

Rodriguez-Fernandez, N.J., Sabater, J.M., Richaume, P., de Rosnay, P., Kerr, Y.H., Albergel, C., Drusch, M., & Mecklenburg, S. (2017). SMOS near-real-time soil moisture product: processor overview and first validation results. *Hydrology and Earth System Sciences*, 21, 5201-5216

Van der Schalie, R., Kerr, Y.H., Wigneron, J.P., Rodríguez-Fernández, N.J., Al-Yaari, A., & de Jeu, R.A.M. (2016a). Global SMOS soil moisture retrievals from the land parameter retrieval model. *International Journal of Applied Earth Observation and Geoinformation*, 45, 125-134

van der Schalie, R., Rodríguez-Fernández, N.J., Kerr, Y.H., Wigneron, J.P., Al-Yaari, A., & de Jeu, R.A.M. (2016b). Passive Microwave Soil Moisture Data Fusion: Final evaluation. In, *ESA report for project IPL-PSO/FF/vb/13.886EXPRO+*: U. Amsterdam